Improving the representation of major Indian crops in the Community Land Model version 5.0 (CLM5) using site-scale crop data

Kangari Narender Reddy[1], Somnath Baidya Roy[1], Sam S. Rabin[2], Danica L. Lombardozzi[2, 3], Gudimetla Venkateswara Varma[1], Ruchira Biswas[1], and Devavat Chiru Naik[4]

[1]Centre for Atmospheric Sciences, Indian Institute of Technology Delhi, New Delhi, 110016, Delhi, India
[2]Climate and Global Dynamics Laboratory, National Centre for Atmospheric Research, Boulder, 80307, CO, USA
[3]Department of Ecosystem Science and Sustainability, Colorado State University, Fort Collins, 80523, CO, USA
[4]Department of Civil Engineering, Indian Institute of Technology Delhi, New Delhi, 110016, Delhi, India

Correspondence to: K. Narender Reddy (knreddy@cas.iitd.ac.in)

Abstract. Accurate representation of croplands is essential for simulating terrestrial water, energy, and carbon fluxes over India because croplands constitute more than 50% of the Indian land mass. Wheat and rice are the two major crops grown in India, covering more than 80% of the agricultural land. The Community Land Model version 5 (CLM5) has significant errors in simulating the crop phenology, yield, and growing season lengths due to errors in the parameterizations of the crop module, leading to errors in carbon, water, and energy fluxes over these croplands. Our study aimed to improve the representation of wheat and rice crops in CLM5. Unfortunately, the crop data necessary to calibrate and evaluate the models over the Indian region is not readily available. This study used comprehensive wheat and rice novel crop data for India created by digitizing historical observations. This dataset is the first of its kind, covering 50 years and over 20 sites of crop growth data across tropical regions, where data has traditionally been spatially and temporally sparse. We used eight wheat sites and eight rice sites from the recent decades. Many sites have multiple growing seasons, taking the tally up to nearly 20 growing seasons for each crop. We used this data to calibrate and improve the representation of the sowing dates, growing season, growth parameters, and base temperature in the CLM5 model. The modified CLM5 performed much better than the default model in simulating the crop phenology, yield, carbon, water, and energy fluxes compared to the site scale data and remote sensing observations. For instance, Pearson's *r* for monthly LAI improved from 0.35 to 0.92, and monthly GPP improved from -0.46 to 0.79 compared to MODIS monthly data. The *r* value of the monthly sensible and latent heat fluxes improved from 0.76 and 0.52 to 0.9 and 0.88, respectively. Moreover, because of the corrected representation of the growing seasons, the seasonality of the simulated irrigation now matched the observations. This study demonstrates that the global land models must use region-specific parameters rather than global parameters for accurately simulating vegetation processes and corresponding land surface processes. The improved CLM5 model can be used to investigate the changes in growing season lengths, water use efficiency, and climate impacting crop growth of Indian crops in future scenarios. The model can also help in providing estimates of crop productivity and net carbon capture abilities of agroecosystems in future climate.

1 Introduction

Land Surface Models (LSMs), the land components of Earth System Models (ESMs), represent a wide variety of processes, including energy partitioning, carbon and mass exchange, and interaction with the hydrological cycle, to name a few. LSMs provide boundary conditions and interact with various components of ESMs (Fisher and Koven, 2020; Strebel et al., 2022). LSMs have come a long way, from a very basic representation of energy budget at the surface level to a very complex state where each grid cell consists of multiple land units and unique interaction of the individual land unit with the atmospheric forcings (Blyth et al., 2021). LSMs use sophisticated parametrization and modules to represent the complex land surfaces and their interactions with other components of ESMs. One important component of LSMs that significantly impacts not only land processes but also atmospheric processes is agricultural land. LSMs strive towards a realistic depiction of agricultural land cover and its processes. Until the last decade, the depiction of crops was mainly constrained to rudimentary models that do not include agricultural practices such as irrigation and fertilization or simply depicted crops as natural grassland (Elliott et al., 2015; McDermid et al., 2017). Enhancements to crop modules gave LSMs a greater capacity to investigate changes in water and energy cycles from croplands and crop yield in response to climate, environment, land use, and land management variations. Recent studies provide valuable insights for enhancing the accuracy of simulating biogeophysical and biogeochemical processes at both regional and global scales in LSMs (Lobell et al., 2011; Osborne et al., 2015; Sheng et al., 2018; Lombardozzi et al., 2020; Boas et al., 2021; Ma et al., 2023).

The Community Land Model (CLM) has, since version 4.0, included a prognostic crop module based on the Agroecosystem Integrated Biosphere Simulator (Agro-IBIS) (Levis et al., 2012; Lawrence et al., 2018; Lawrence et al., 2019). This module can simulate the soil-vegetation-atmosphere system, including crop yields. The most recent version of CLM, CLM5, is a leading land surface model with an interactive crop module representing crop management. The module comprises eight crop types that are actively managed: temperate soybean, tropical soybean, temperate corn, tropical corn, spring wheat, cotton, rice, and sugarcane. It also contains irrigated, non-irrigated, and unmanaged crops (Lombardozzi et al., 2020). Currently, CLM5 is the sole land surface model incorporating dynamic spatial patterns of significant crop varieties and their management (Lombardozzi et al., 2020). Although CLM5 showed advancements compared to its previous versions, limited research conducted at the point and regional scales indicates that it may provide poor phenology and yield predictions for specific crops (Chen et al., 2018; Sheng et al., 2018; Boas et al., 2021). The energy and carbon fluxes are highly affected by inaccuracies in crop phenology, particularly concerning the timing of planting and harvesting.

The Indian subcontinent is a significant landmass that significantly affects the earth system energy, water, and carbon fluxes. Nearly 50% of the land cover is used for agriculture in India, and two major cereal crops, wheat and rice, occupy nearly 80% of the total agricultural land. However, CLM5 simulations of rice and wheat over the Indian subcontinent show large biases in simulating annual crop yield (Lombardozzi et al., 2020). The major growing seasons of wheat and rice are the rabi and kharif seasons, but CLM5 grows wheat and rice in the summer and rabi seasons, respectively. The irrigation patterns simulated by CLM have a bias in seasonality, which Mathur and AchuthaRao. (2019) highlighted. Irrigation is an essential feature of the

croplands in India, especially during the rabi season (Gahlot et al., 2020) for wheat and in dry regions for rice. Therefore, the bias in irrigation points to the lack of accurate representation of Indian crops.

Gahlot et al. (2020) used an LSM (Integrated Science Assessment Model; ISAM) to investigate the wheat croplands of India. The major drawback of the study was the lack of enough site-scale observations to calibrate and validate the model while covering the broad growing conditions of India. Therefore, in this study, we aim to investigate and improve the representation of major Indian crops—wheat and rice—in the latest version of CLM (CLM5.0). We used site-scale observations from multiple sites to calibrate the parameters essential for the crop module in CLM5 and evaluate the model. The site-scale observations cover various climatic conditions experienced by crops in India, thus making this a robust calibration of an LSM. Further, we aimed to quantify the impacts of realistic representation of Indian crops on various land processes such as irrigation, gross primary production, latent heat, and sensible heat.

The current paper is structured as follows: First, we briefly describe the CLM5 model and the site scale data used in this study. Then, we describe the shortcomings of CLM5 in simulating Indian crops, comparing them to the observations. Next, we dive into the need for modifications in CLM5 and the changes made to parameters and the source code of the CLM5. The results section compares our improved model at site and regional scales. We compare the CLM5 simulations against observed Leaf Area Index (LAI), yield, and growing season length at site scale. At the regional scale, we compare against yield, irrigation patterns, LAI, Gross Primary Production (GPP), Latent Heat flux (LH), and Sensible Heat flux (SH) observations. Finally, we discuss the impact of the study and the conclusions.

2 Materials and Methods

2.1 Community Land Model version 5 (CLM5.0)

CLM5 is the latest version of the land component in the Community Earth System Model (CESM) (Lawrence et al., 2018, 2019). The biogeochemistry mode of CLM5 (CLM5-BGC) is widely used to estimate the water, energy, and carbon fluxes in various climatic zones (Cheng et al., 2021; Denager et al., 2023; Song et al., 2020; Seo and Kim, 2023). The biogeochemistry and crop module of CLM5 (BGC-Crop) is modified in various studies to meet regional constraints, and the resulting impact on various fluxes is analyzed (Boas et al., 2021; Raczka et al., 2021; Boas et al., 2023; Yin et al., 2023). Studies show that incorporating agriculturally managed land cover can improve the general representation of biogeochemical processes (Boas et al., 2021). The CLM5 crop module includes new crop functional types, updated fertilization rates and irrigation triggers, a transient crop management option, and some adjustments to phenological parameters (Lombardozzi et al., 2020).

CLM5 has a better representation of the land surface by using a tile representation. This allows the model to have various land types inside a grid cell. In its latest version, the model supports 79 plant functional types with 32 rainfed and 32 irrigated crop types. The complex representation of the land surface makes CLM5 a better model on various metrics tested by International Land Model Benchmarking (ILAMB) (Collier et al., 2018).

The current study used the CLM5 model in the data atmosphere mode, i.e., not interacting with the atmosphere. The GSWP3 atmospheric data is used for the simulations. We ran CLM5 at two different spatial resolutions from 2000 to 2014: site-scale

simulations to calibrate the crop module and regional simulations to evaluate the calibrated model against remote sensing data and derived surface flux data (Sect. 2.5). The plant functional type of the crops in CLM5 considered in this study are wheat (19: rainfed and 20: irrigated) and rice (61: rainfed and 62: irrigated). The default CLM5 model is referred to as CLM5_Def throughout this paper. CLM5_Mod1 and CLM5_Mod2 are the two setups of the model developed in this study, and they are described in detail in Section 2.3. The overall methodology and steps followed in this study are depicted as a flowchart (Figure S1) and explained in detail in the following sections.

2.1.1 Site scale simulations

For site scale simulations, we created domain, surface, and land use time series data for the respective sites (for details on sites, Section 2.2 and Figure 1). The resolution of the data is 0.1° and has one grid cell with the site at its center. The method used to generate the data is available in the documentation of Reddy et al. (2024). The domain file represents the spatial extent of our simulation. The surface data represents the local soil and surface properties. The land use time series reflects the varying land-use land cover change from 1850 to 2015 at sites. Spin-up at each site is carried out for 200 years in accelerated deposition mode (AD mode) and 400 years in normal mode. The GSWP3 atmospheric data is used for the site scale simulations.

2.1.2 Regional-scale simulations

For regional scale simulations, we fixed the domain between 60 °E to 100 °E and 0 °N to 40 °N (Figure S2), covering the Indian subcontinent. The domain, surface, and land use time series data are generated for the domain mentioned above with a spatial resolution of 0.5° (files available at Reddy et al., 2024). The spin-up for the regional case is carried out in two stages. Two hundred years of spin-up in AD mode and 400 years in normal mode. The simulation data at the end of 400 years is used as initial conditions for our regional simulations. The regional simulations are run from 1995 to 2014, and the data from 2000 to 2014 is used for the analysis. The GSWP3 atmospheric data is used as atmospheric forcing for the regional scale simulations.

2.2 Site scale crop data

Site-scale data of the type and quality required for calibrating and validating crop models are not readily available in India. This is unfortunate because plenty of data has been collected, but they have never been properly archived. India has invested heavily in agricultural studies and has built nearly 70 agricultural institutes nationwide since the green revolution in the 1960s, with each state having at least one institute dedicated to studying regional crops. Master's and PhD student theses from these institutes, many containing site-scale observations, were recently consolidated and brought into the public domain in the KrishiKosh repository (Veeranjaneyulu, 2014). However, the data is complex to extract from these theses because of the data collection and reporting structure differences followed by various institutes. For this study, we assembled data on wheat and rice in a formatted, machine-readable format that can be downloaded and used for model development. The data is available on the PANGEA repository (Varma et al., 2024). We used the site scale data (years 2000 to 2014) generated by Varma et al. (2024) to evaluate our CLM5 model (Table S1 and Figure 1).

2.3 Improvements in CLM5

The parameters impacting planting and growing stages in CLM5 are minimum and maximum planting dates, minimum planting temperature, planting temperature, base temperature for Growing Degree-Day (GDD) calculations, minimum GDD

for crop emergence, and GDD threshold for crop grain fill. The minimum planting temperature and the average minimum planting temperature of the growing season govern the planting date of the crop in CLM5. The base temperature defines the crop growth rate and the accumulation of GDD. Crop growth has different phases: emergence, flowering, grain fill, and maturity. The CLM5 model simulates the crop growth phases using the accumulated GDD. Therefore, base temperature becomes a critical parameter that defines the crop growth in CLM5. The base temperature and maximum GDD control the longevity of each phase in crop growth. The allocation to the grain starts once the crop reaches the grain fill stage, which is controlled through the "grnfill" parameter in CLM5. The "grnfill" parameter defines the threshold for initiating the grain-filling stage as a fraction of the GDD required for maturity (hybgdd in Table 1). Growing season length in CLM5 is directly controlled through base temperature. The lower the base temperature, the faster the GDD accumulation and the shorter the growing season length. The planting window, base temperature, GDD required for maturity, and grain fill parameters have a significant impact on crop growth and are considered widely when calibrating the crop module in CLM5 (Fisher et al., 2019; Cheng et al., 2020; Boas et al., 2021).
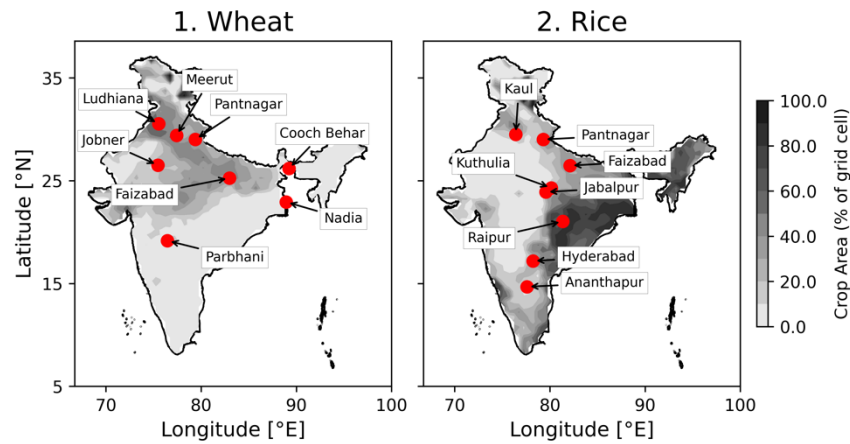
Figure 1: Location of sites used in the current study for calibrating and validating the major Indian crops (1) Wheat and (2) Rice. The contour map shows the percent of crop area in each 0.5° grid cell.

The improvements to the wheat and rice crops in CLM5 are made in two steps. We first perform a literature survey and conduct sensitivity experiments to find the best-performing parameters shown in Table 1 (Section 2.3.1). The CLM5_Mod1 setup is the result of the new parameter values. Second, we calibrate the latitudinal variation in base temperature through sensitivity experiments (Section 2.3.2). The CLM5_Mod2 setup results from calibrating the latitudinal variation in base temperature. Changes in the source code of CLM5 were necessary to facilitate the incorporation of changes made to parameters (see Section 2.3.1.1).

2.3.1 Improvements in CLM5_Mod1

2.3.1.1 Wheat

155 CLM5_Def simulated the wheat growth from April to August. This starkly contrasts with ground reality, where Indian farmers sow wheat in late October to early November and harvest in late March or April (rabi season) (Sacks et al., 2010; Gahlot et al., 2020). To implement a realistic growing season, we performed sensitivity simulations by varying the planting window of 45 days, from mid-October to late November (see Table S2). The planting window shown in Table 1 produced the best results in lowering the bias in simulated LAI, yield, and growing season length and, therefore, is used in CLM5_Mod1. The

160 CLM5_Def base temperature for wheat is 0 °C, but during our literature survey, we found the optimal base temperature for wheat in India is 5 °C (Mukherjee et al., 2019; Mehta and Dhaliwal, 2023). The planting temperature threshold in CLM5 for wheat is low compared to observations in India (Rao et al., 2015; Asseng et al., 2016; Mukherjee et al., 2019). The grain fill threshold of 0.6 for wheat performed well amongst tested values in our sensitivity studies (Table S2), and therefore, we did not change the parameter value.

165 **2.3.1.2 Rice**

CLM5_Def simulated rice growth from January to May. In contrast, rice is grown in India during the monsoon season due to the high-water requirements of the rice crop. Rice is sown in the last week of June to early July and harvested at the end of October and early November, also known as the Kharif season. Many regions in India grow rice during the summer and rabi seasons, which meet their water requirements mainly through irrigation. The rice crop area grown in summer and rabi is very

170 low compared to the rice crop grown in the kharif season (Biemans et al., 2016). Therefore, we confined ourselves to the major rice growing season (kharif season) to calibrate the model. A sensitivity study is conducted with a planting window of 45 days, from early June to late July (Table S2). The planting window shown in Table 1 for rice gave the best results. The base temperature used for rice crop (10 °C) in CLM5_Def is the same as that observed in the literature for the Indian region (Thakur et al., 2022). However, we found that the planting temperature observed in India differs from those used in CLM5_Def (Jat et

175 al., 2019; Kumar et al., 2023). The grain fill threshold used for rice in the CLM5_Def case resulted in very poor LAI and yield simulations, which was earlier recognized by Lu and Yang (2021) while studying rice in China using CLM. Through a sensitivity test, we found that the grain fill threshold of 0.65 performed the best in simulating LAI and yield for rice amongst the tested grain fill values in Table S2.

The parameter of growing degree-days required for maturity (hybgdd) in both wheat and rice was performing well during our

180 sensitivity simulations, and, therefore, its value is not altered. Table 1 shows all the parameters changed in the default CLM5 to improve wheat and rice crop growth for the Indian region.

Table 1: Parameter values for wheat and rice in the CLM5 crop module

Parameter	Description (units)	Wheat		Rice	
		CLM5_Def	CLM5_Mod1	CLM5_Def	CLM5_Mod1
min_NH_planting_date	Minimum planting date for the Northern Hemisphere (MMDD)	401	1115 (calibrated in this study)	101	701 (calibrated in this study)
max_NH_planting_date	Maximum planting date for the Northern Hemisphere (MMDD)	615	1231 (calibrated in this study)	228	815 (calibrated in this study)

min_planting_temp	Average 5-day daily minimum temperature needed for planting (K)	272.15	283.15 (Rao et al., 2015)	283.15	294.15 (Kumar et al., 2023)
planting_temp	Average 10-day temperature needed for planting (K)	280.15	290.15 (Asseng et al., 2017; Mukherjee et al., 2019)	294.15	300.15 (Jat et al., 2019)
baset	Base Temperature (°C)	0	5 (Mukherjee et al., 2019; Mehta and Dhaliwal, 2023)	10	10 (Thakur et al., 2022)
grnfill	Grain fill parameter	0.6	0.6	0.4	0.65 (calibrated in this study)
hybgdd	Growing Degree Days for maturity (°C-days)	1700	1700	2100	2100
baset_mapping	Switch to turn on/off the latitudinal variation in baset in the tropics	'constant'	'constant'	'constant'	'constant'

2.3.1.4 Source code changes

185 Along with the parameter changes, we had to change the model source code to fix a bug with northern-hemisphere crop seasons that start in one calendar year and finish in the next. The code added to the module CNPhenologyMod.F90 begins at line 2001 (Supplementary text S1). The code changes are available at Reddy et al. (2024).

This bug is fixed in more recent versions of CLM, starting with tag ctsm5.1.dev131. A bug was also fixed to make CLM use user-specified values of parameters latvary_intercept and latvary_slope, which allow latitudinal variation of base temperature.

190 More recent versions of CLM, starting with tag ctsm5.1.dev155, include this fix.

2.3.2 Mod2 case parameters: Varying base temperature by latitude

CLM5 can vary CFT base temperature by latitude to account for cultivars bred for optimal performance in different climates. Currently, only wheat and sugarcane have these capabilities turned on. We extended this latitudinal variability to rice and improved the existing one for wheat in India. The latitudinal variation in base temperature is defined by two parameters:

195 latvary_intercept and latvary_slope. The equation in the model that uses these parameters is:

$$Tbase_{lat} = Tbase + latvary_{intercept} - \min\{latvary_{intercept}, latvray_{slope} * |latitude|\} \dots\dots(1)$$

latvary_slope and *latvary_intercept* define the latitudinal extent of the base temperature variation. *Tbase* refers to the base temperature used for GDD calculation beyond the latitudinal limit.

We conducted sensitivity studies to find the optimal latvary_intercept and latvary_slope values for wheat and rice. We ran the

200 site scale simulations at experimental sites and compared the model estimates against the LAI, yield, and growing season-length observational data. This resulted in 14 sites in total (Table S1), 7 for rice and 8 for wheat. Bias is considered to calibrate the model. The bias formula used in the study is:

$$Mean\ Absolute\ Bias\ (MAB) = \frac{\sum|CLM_{var} - Obs_{var}|}{\sum(Obs_{var})} \dots\dots(2)$$

where *var* is LAI, yield, or growing season length.

MAB is calculated for LAI, yield, and growing season length. The overall bias, used as our evaluation metric during calibration, is calculated as the equally weighted average of mean absolute bias in LAI, yield, and growing season length.

We ran ten simulations at each site to test the sensitivity of base temperature on crop growth and evaluate optimal base temperatures. Two simulations, CLM5_Def and CLM5_Mod1, use the parameter values shown in Table 1. The other eight simulations at each site used the same parameter set as given in Table 1 but with a base temperature (based) changed relative to the CLM5_Mod1 values given thereby $\pm$ [1, 2, 3, 4] °C. The total number of site scale simulations conducted and used for this sensitivity analysis is 150 (15 sites, 10 simulations per site). These simulations helped us understand the bias in the CLM5_Def and CLM5_Mod1 simulations and the sensitivity of base temperature on crop growth and phenology at individual sites.

Figure 2 represents the sensitivity of wheat and rice crop growth to base temperature in the site-scale sensitivity simulations. The y-axis depicts the overall bias in the model (sum of bias in LAI, yield, and the growing season length). In the case of wheat, the CLM5_Def parameterization has the highest bias at all sites in the range 0.45-0.8 (markers in dark green color in Figure 2(a)). The bias in CLM5_Mod1 is in the range of 0.1-0.3 (markers in light green in Figure 2(a)). The bias in sensitivity experiments with the base temperature at each site is shown in Figure 2 with grey markers, and the least biased simulation at each site is shown in black marker. The base temperature of 5 °C produced the least bias at three sites (Pantnagar, Meerut, and Jobner). The remaining four sites have the least bias at temperatures above 5 °C. Ludhiana site, which is above 30 °N, performed the best at 6 °C, while Parbhani, Cooch Behar, and Faizabad had the least bias at 7 °C. The three sites having the least bias at 7 °C are in the central and southern parts of the wheat-growing regions of India. The sites performing best at 5 °C are in the northern part of the wheat-growing region.

In the case of rice, CLM5_Def has the highest bias, ranging from 0.5-0.95 (shown in dark green markers in Figure 2(b)). The difference between the CLM5_Def and CLM5_Mod1 cases is the grain fill parameter (Table 1). Using 0.65 as grain fill drastically improved the rice crop simulations. The bias in CLM5_Mod1 is in the range of 0.1-0.3 (markers in light green in Figure 2(b)). All the sensitivity experiments used the grain fill parameter of 0.65. The sensitivity of base temperature in rice showed that the sites in the southern rice growing regions (lower than the Tropic of Cancer, latitude < 23.5 °N) have the least bias at 11 or 12 °C. The sites in the central rice growing regions (23.5 °N < latitude < 29 °N) have the least bias while using base temperatures of 8 or 9 °C. Finally, the sites towards the country's northern parts (latitude > 29 °N) perform best at 9 °C as the base temperature. Therefore, not all sites perform optimally at a single base temperature, and a latitudinal variation in base temperature can improve the rice crop simulations.

The base temperature at which the least bias is observed at each site and the corresponding latitude is noted for wheat and rice crops (Table S3). Using the ordinary least squares method, the values for latvary_intercept and latvary_slope are calculated, satisfying Eq. (1) for wheat and rice (Table 2 and Figure S3). Figure S3 shows the linear fit of the base temperature at which the lowest bias is observed (Table S3) and the latitude of the site. The linear fit has a high R^2 of 0.64 for wheat and 0.68 for rice.
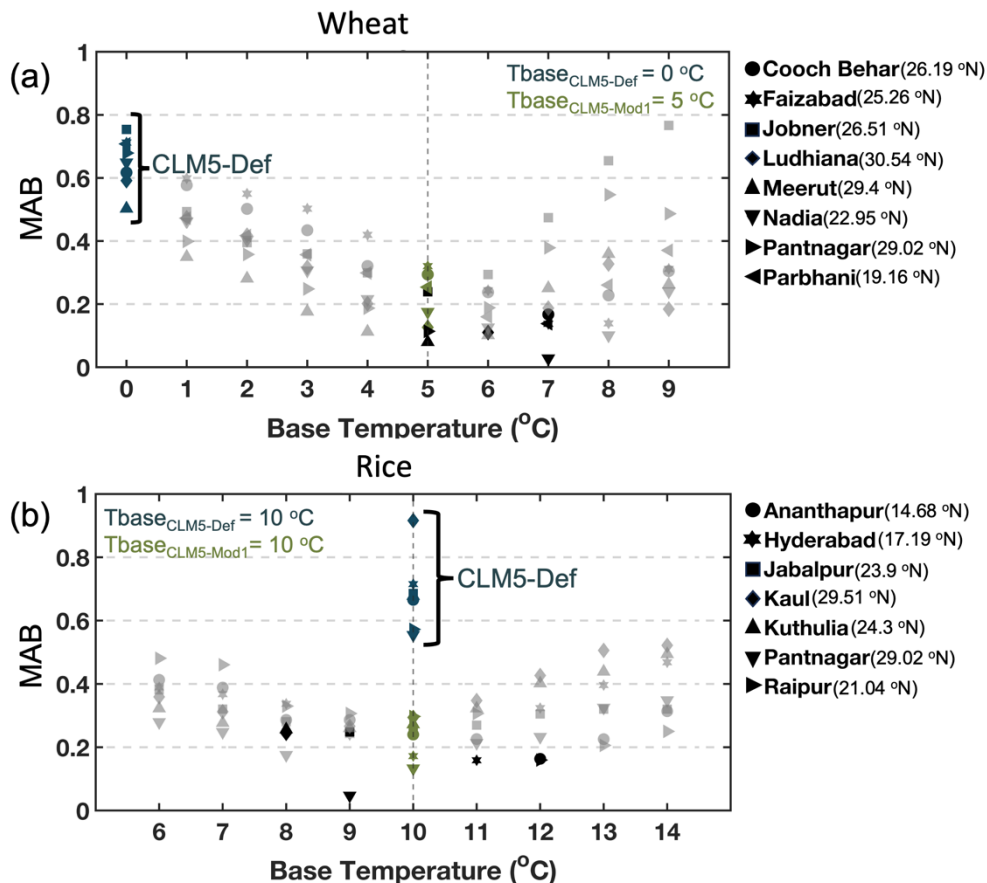
Figure 2: The overall bias in the site scale simulations during the sensitivity study of base temperature (x-axis) for (a) spring wheat and (b) rice. The y-axis shows the overall bias (mean of absolute bias in LAI, yield, and growing season length). The dark green markers show the bias in the Def case at a site, the light green marker shows the bias in the Mod1 case at a site, and the black marker shows the lowest bias simulated at a site. The grey markers show the bias simulated in the sensitivity study of base temperature at a site. The legend shows the name and latitude of the sites.

The Mod2 version of the model used these parameters. In CLM5_Mod2, we used the baset_mapping equal "varytropicsbylat" in the CLM namelist to turn on the latitudinal variation in base temperature in the model. To incorporate the latitudinal variation for rice crops in CLM5, an addition to the code of CropType.F90 is made at line 602 (see supplementary material).

Table 2: Latitudinal variation parameters for wheat and rice

Parameter name	Wheat		Rice	
	CLM5_Def	CLM5_Mod2	CLM5_Def	CLM5_Mod2
baset	0	5.4*	10	9*
latvary_intercept	12	6*	NA	6.8*
latvary_slope	0.4	0.19*	NA	0.26*

* significant at p<0.05 using the t-statistic of the two-sided hypothesis test. NA – Not Applicable

2.4 Evaluation metrics

250 The comparison of CLM5 simulations with observations at site scale and regional scale used four evaluation parameters: mean absolute bias (MAB) (Eq. 2), root mean square error (RMSE), Pearson's *r*, and Kling-Gupta Efficiency (KGE, Gupta et al., 2009). MAB is the normalized deviation from the observations, with values close to 0 indicating good performance. RMSE is the mean deviation of model simulations from observations. Pearson's *r* gives the correlation between the model estimates and observations. KGE (Eq. 3) offers a diagnostic insight into the model performance because it is a composite of correlation, bias,

255 and variability.

$$KGE = 1 - \sqrt{(r-1)^2 + (\beta-1)^2 + (\gamma-1)^2} \quad \text{.... Eq. (3)}$$

$$\beta = \frac{\mu_{CLM}}{\mu_{Obs}}$$

$$\gamma = \frac{\sigma_{CLM}}{\sigma_{Obs}}$$

where KGE is the Kling-Gupta Efficiency, *r* is the Pearson's coefficient between CLM simulated variable and observations, β

260 is the bias ratio (ratio of means-μ of the modeled and observation values) and γ is the variability ratio (ratio of standard deviations- σ of modeled and observation values). KGE, *r*, β, and γ have their optimum at unity.

KGE is widely used in hydrological modeling because of its easy formulation and interpretation (Kling et al., 2012). KGE also makes sense from an agroecosystem point of view because we are interested in reproducing temporal dynamics, as well as preserving the spatial variation in crop growth caused by diverse climatic conditions in the Indian region, which are given by

265 the first (β) and the second (γ) moments, respectively.

Taylor's diagram (Taylor, 2005) is used to assess the CLM5 model. The Taylor diagram summarizes the relative skill with which different models imitate the pattern in observations. The three versions of the CLM5 model from the study are represented by triangles on the Taylor diagram (Figure 10). The distance between each CLM5 setup and the point displayed as a black star (observation data) on the Taylor diagram indicates how accurately each model reproduces observations. Three

270 statistics of the simulated fields are plotted on the Taylor diagram: a) the centered RMS error that is proportional to the distance from the point on the x-axis shown as a black star (dark green contours); b) the standard deviation that is proportional to the radial distance from the origin (grey semi-circular contours); and c) the Pearson correlation coefficient that is proportional to the azimuthal angle (light grey contours). Higher correlation, lower RMS error, and smaller standard deviation characterize the most accurate CLM5 configuration.

275 **2.5 Model evaluation at the site scale**

We compared the CLM5_Def, CLM5_Mod1, and CLM5_Mod2 simulations against the site-scale observations. We evaluated three crop variables: LAI, growing season length, and yield. We used four evaluation metrics: MAB, RMSE, Pearson's *r*, and KGE (described in Section 2.4). Because the count of observation data points is low, we used the bootstrapping method to estimate the significance of improvement from CLM5_Def to CLM5_Mod1 and CLM5_Mod1 to CLM5_Mod2.

280 Bootstrapping is carried out with 10000 samples for each evaluation metric, and the Student's T-test is conducted to check if

each model improvement performs significantly better (p<.05) than its predecessor. Table 3 shows the above-mentioned evaluation metrics. Note that 64% of the observations are used for calibration, and the rest marked with "*" in Table S1 are used for validation.

2.6 Model evaluation at the regional scale

2.6.1 Yield

We compared the yield simulated by CLM5 against the EarthStat yield data (Ray et al., 2012) retrieved from the "Harvested Area and Yield for 4 Crops (1995–2005)" dataset. EarthStat yield data is available at a spatial resolution of 0.1°x0.1° and is given as a five-year average. In this study, we used the 2005 EarthStat data (representing the average yield from 2003 to 2007) regridded to 0.5°x0.5° and compared it against the CLM5 simulated yield data averaged from 2003 to 2007.

2.6.2 Irrigation

An investigation on irrigation using a climate model in Indian croplands was carried out by Biemans et al. (2016). The study highlighted the necessity of improving the cropping patterns to improve the irrigation patterns. We compared the annual mean irrigation pattern simulated by three versions of CLM5 against the annual mean irrigation water demand for wheat and rice from Biemans et al. (2016). The irrigation pattern data from Biemans et al. (2016) was unavailable as a supplement. Therefore, we extracted data from the Figure 5 of Biemans et al. (2016).

2.6.3 LAI and GPP

We compared the regional scale model simulations against the Moderate Resolution Imaging Spectroradiometer (MODIS) 8-day GPP (MOD17A2HV006) (Running and Zhao, 2015) and LAI (MOD15A2HV0061) (Myneni et al., 2021). GPP and LAI data was retrieved from the Integrated Climate Data Centre (ICDC) website (http://icdc.cen.uni-hamburg.de/las/). The MODIS GPP and LAI data mostly have four observations per month. We took the average of the observations in a month and compared them against the monthly averaged CLM5 data. We compared the MODIS monthly spatial observations with corresponding CLM5 simulations from 2001 to 2014. This exercise is to observe the spatial variation in LAI and GPP over the Indian region. We also compared the spatially averaged time series of monthly LAI and GPP over the Indian subcontinent from 2001 to 2014. This exercise is to compare the inter annual cycle in MODIS observations and CLM5 simulations.

2.6.4 Latent and Sensible Heat Flux

For the evaluation of changes in surface energy fluxes, we used the FLUXCOM data (Tramontana et al., 2016; Jung et al., 2019). FLUXCOM data is generated using machine learning to merge the flux measurements in eddy covariance towers with remote sensing and meteorological data and estimate surface fluxes (Jung et al., 2019). We used the monthly 0.5° resolution RS_METEO version of the FLUXCOM data for comparison against the CLM5 simulations. We compared the monthly spatial average of heat fluxes against CLM5 simulations. We also compared the inter-annual time series of heat fluxes with the CLM5 simulations.

3 Results

3.1 Outcomes of model improvements at site scale

3.1.1 Wheat

3.1.1.1 LAI

The Leaf Area Index (LAI) impacts biomass accumulation and transpiration process, while biomass distribution directly affects the yield. Furthermore, LAI is crucial in modeling multiple processes, including evapotranspiration and canopy photosynthesis. Additionally, the contact between the plant and the atmosphere is crucial in estimating the transfer of energy and matter between the canopy and the atmosphere (Su et al., 2022). Therefore, LAI is the most important of the three variables evaluated here.

Figure 3 depicts the time series of LAI simulated by the three different versions of CLM5 for different sites. Results show that CLM5_Def simulated wheat growth during April-June while CLM_Mod1 and CLM_Mod2 simulated wheat growth in November-March. The CLM5_Def simulated the wheat growth in the wrong season compared to observations. Furthermore, CLM5_Def also underestimated LAI. The seasonality error is corrected in CLM5_Mod1 with the change in the sowing window (min_ and max_NH_planting_date in Table 1), but it still underestimated LAI. Including latitudinal variation in base temperature in the CLM5_Mod2 case improved the LAI simulation by reducing the underestimation in most sites except Cooch Behar (Figure 3(a) and 3(b)), Faizabad (Figure 3(c), 3(d) and 3(e)), and a few growing seasons in Naida (Figure 3(o)). Overall, CLM5_Mod2 provided the best estimates of LAI (Fig. 4).

Table 3 shows the impact of improvements made to the CLM5 model. The observed mean maximum LAI is 4.22 m^2/m^2. CLM5_Mod2 is the closest to the observation with a value of 3.47 m^2/m^2, while CLM5_Def is the worst with a value of 2.36 m^2/m^2. Figure 3 shows us that the crop in the CLM5_Def case grows in the wrong season compared to what is observed. Hence, all performance metrics for the LAI simulations in the CLM5_Def case will show very poor results because the simulated LAI values are all zero during the observed growing season. To ensure a fairer comparison between the CLM5_Def and CLM5_Mod cases, we used days from sowing instead of calendar dates in the LAI time series. Even after adjusting for the growing season, the LAI in the CLM5_Def case has a large MAB of 0.81. The CLM5_Mod1 and CLM5_Mod2 performed much better with MABs of 0.52 and 0.43. The negative r-value for LAI in the case of CLM5_Def is due to the simulation of smaller growing lengths and having zero LAI values when the observations reach their maximum values. The r-value improved in both the Mod cases, with a higher *r*-value of 0.3041 (significant at p<.01) in the CLM5_Mod2 case. KGE value is a good measure of how the model is performing both in seasonality and spatially. KGE for CLM5_Def is very low (-0.62). CLM5_Mod1 showed improvement with a value of -0.02, but it is still negative. CLM5_Mod2 has the highest value of 0.19.

Figure 4 shows the CLM5 model performance in simulating crop growth at each site. The larger the marker size, the higher the bias simulated at that site. The three model versions are shown in three distinct colors, red representing CLM5_Def, cyan representing CLM5_Mod1, and blue representing CLM5_Mod2. The improvement in LAI simulations is evident from Figure 4(a.1). The LAI simulations in Mod cases have a lower bias (smaller and the top marker) compared to the CLM5_Def case.

The improvement in model simulation is not uniform across the wheat-growing region. A more significant improvement is seen in Ludhiana, Meerut, and Pantnagar, which belong to the most fertile and well-irrigated regions of India. Jobner and Parbhani also saw considerable improvement from CLM5_Def to CLM5_Mod2. These two sites belong to regions with limited water supply. The introduction of latitudinal variation has drastically improved the simulation at Ludhiana, Meerut, Pantnagar,

Jobner, Nadia, and Parbhani, all belonging to distinct agro-climatic regions, proving the robustness of the model and the
350 importance of varying base temperatures for better crop simulation.

Overall, the modified models significantly improved over the default model, with CLM5_Mod2 performing the best (Table 3 and Figure S4).
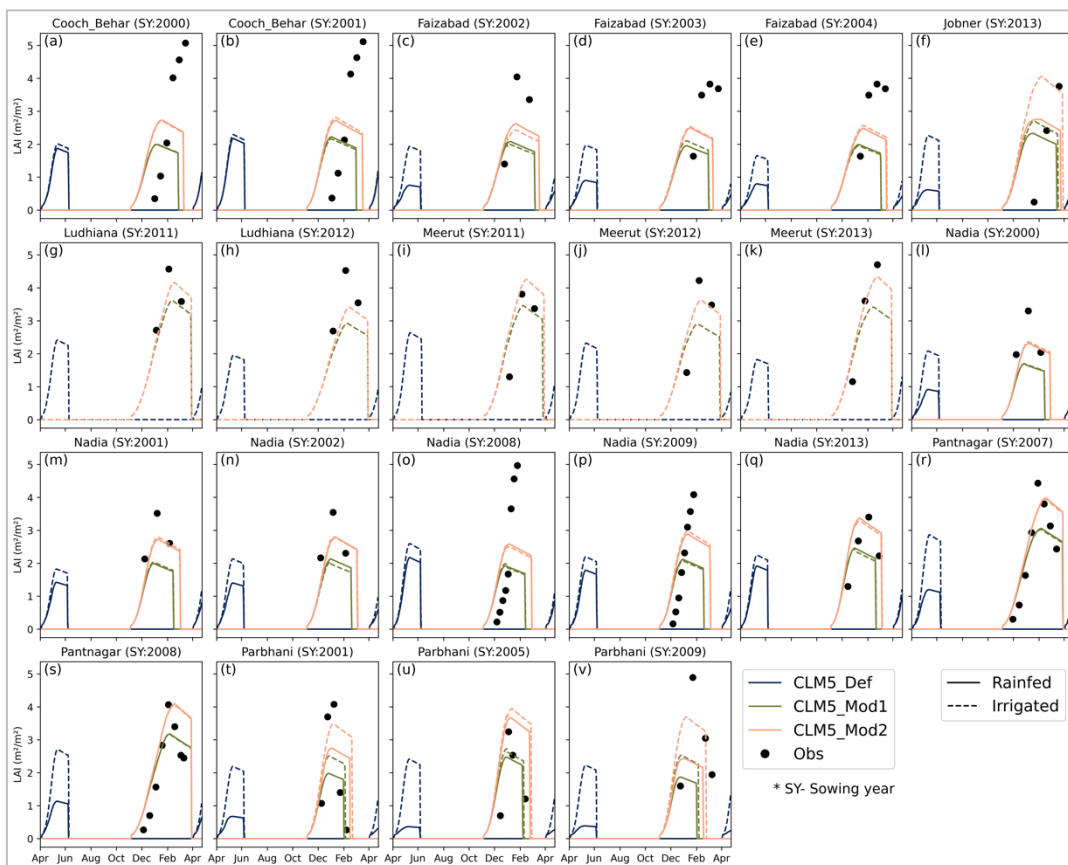
Figure 3: Site scale LAI simulated by three versions of CLM5 against observations for wheat.

355 **3.1.1.2 Yield**

The observed mean yield is 3.88 t/ha (Table 3). The default model underestimated the mean yield with a value of 3.05 t/ha. The modified models performed better, simulating a mean yield of 3.68 t/ha across all sites. All metrics in Table 3 show that the default model is the worst performer with high MAB and RMSE and low correlation and KGE values. The CLM5_Mod1 is the best performer in all metrics (bold text). It is important to note that CLM5_Mod2 performs quite well. The mean yields

360 of CLM5_Mod1 and CLM5_Mod2 are identical, and the correlation values of 0.38 in CLM5_Mod1 and 0.30 for CLM5_Mod2 are not statistically different (significance level, $p<.05$).

Site scale comparison of wheat yield (Figure 4(b.1)) highlights that the yield simulated in CLM5_Def has high bias at all sites. The high bias in most regions is reduced by improved growing season (CLM5_Mod1) and Tbase (CLM5_Mod2). Cooch

Behar, Faizabad, and Naida all saw improvement in wheat yield simulation from CLM5_Def to CLM5_Mod1 to CLM5_Mod2

365 (Figure 4(b.1) and Figure S5). However, sites in southern (Parbhani) and northern regions (Ludhiana, Meerut, and Pantnagar) improved from CLM5_Def to CLM5_Mod1 but did not improve from CLM5_Mod1 to CLM5_Mod2 (Figure 4 (b.1) and Figure S5). The latitudinal variation in base temperature showed improvements at the sites in central wheat growing regions, while the sites in southern and northern regions did not improve over CLM5_Mod1 (Figure 4(b.1)).
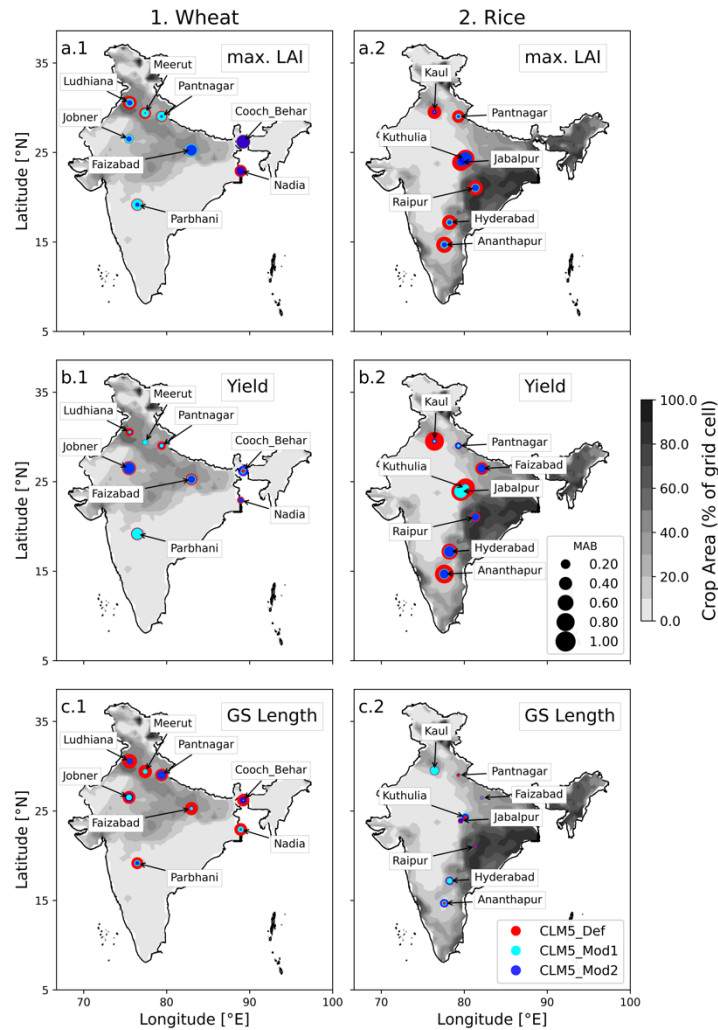
370 **Figure 4: Site-scale CLM performance against observations (1) Wheat; (2) Rice. Crop variables compared are (a) max. LAI during the growing season, (b) yield, and (c) growing season length. The three markers at each site location show the MAB of CLM5_Def (red color), CLM5_Mod1 (cyan color), and CLM5_Mod2 (blue color). The MAB ranges from 0 to 1. The contour on the map is the crop area per 0.5° grid cell.**

3.1.1.3 Growing Season Length

375 The growing season length simulated by CLM5_Def is very low, with a mean growing season of just 69 days, compared to 129 days in observations (Table 3). The growing season length considerably increased to 126 days in CLM5_Mod1 and 136

days in CLM5_Mod2. The MAB in the growing season length in CLM5_Mod1 and CLM5_Mod2 are 0.11 and 0.10, respectively, much lower than the 0.47 in the CLM5_Def case. Incorrect growing season and a lower T_{base} for wheat have led to a very low growing season length simulation in the CLM5_Def. The modified models performed significantly better than the default in terms of all the evaluation metrics (Table 3). Their performances are comparable, with no statistically significant difference ($p<0.05$) between the metrics.

Figure 4(c.1) shows the MAB in growing season length simulation by three CLM5 models across the sites in various climatic conditions. CLM5_Def has the largest bias, performing poorly at all sites (large red markers in Figure 4(c.1)). With the improvements made in CLM5_Mod1, the growing season length simulation has considerably improved at all sites. The changes made in CLM5_Mod2 showed mixed results. Growing season length simulation in CLM5_Mod2 improved over CLM5_Mod1 at Parbhani, Nadia, Pantnagar, and Ludhiana (Figure 4(c.1)). Ludhiana and Pantnagar belong to very fertile regions with very low water stress. Nadia belongs to the delta region, and Parbhani belongs to an arid region. CLM5_Mod2 simulations did not show a considerable improvement over CLM5_Mod1 at Cooch Behar, Jobner, and Meerut.

The results in wheat showed that both the LAI and growing season length significantly improved CLM5_Mod2 over CLM5_Mod1. Table S4 expands on the results discussed above to show the improvements observed during the calibration and validation stages separately. Based on the overall bias in Table 3, Table S3 and Figure S4, we find that wheat simulation improved largely from default to Mod2.

3.1.2 Rice

3.1.2.1 LAI

A significant improvement in LAI rice simulations can be seen in Figure 4(b.2), Figure 5, and Table 3, especially after introducing the latitudinal variation in base temperature. CLM5_Def underestimated the mean maximum LAI with a value of 1.65 m^2/m^2, much lower than the observed 5.29 m^2/m^2 (Table 3). The modified models perform much better, simulating maximum LAI in the range of 4.45-4.5 m^2/m^2. We compared the CLM5 simulated LAI against the observations after correcting the difference in the growing season in CLM5_Def, as discussed in Section 3.1.1.1. The MAB reduced from 0.66 in the CLM5_Def case to 0.387 in the CLM5_Mod1 case to 0.343 in the CLM5_Mod2 case. CLM5_Mod2 LAI performed better than CLM5_Mod1 in other metrics- RMSE, r-value, and KGE (Table 3), and the improvement is significant at $p<.05$.

Figure 4(a.2) shows the LAI simulation of rice by three versions of the model. The bias markers at each site clearly show that the changes made to the model in CLM5_Mod1 and CLM5_Mod2 significantly reduced the bias in maximum LAI simulated during a growing season. CLM5_Mod2 simulations performed better in sites in southern (Figures 5(a), 5(b), and 5(c)) and the northern parts of India (Figures 5(g), 5(i), and 5(j)). The observed model improvements strongly suggest that latitudinal variation in base temperature implemented in the CLM5_Mod2 is essential to capture the growth variation in LAI observed across Indian rice growing regions (Figure 4(a.2) and Figure S4).

Table 3: Evaluation of wheat and rice across three CLM5 setups at site scale

Parameter	Evaluation Metrics	Wheat				Rice			
		Obs	CLM5_Def	CLM5_Mod1	CLM5_Mod2	Obs	CLM5_Def	CLM5_Mod1	CLM5_Mod2
LAI (m²/m²)	Mean of max. LAI	4.22	2.36	2.69	**3.47**	5.29	1.65	**4.48**	4.45
	MAB	--	0.81	0.52	**0.43**	--	0.66	0.39	**0.34**
	RMSE	--	2.61	1.76	**1.41**	--	3.00	1.94	**1.68**
	r	--	-0.45*	0.11	**0.30***	--	0.34*	0.34*	**0.43***
	KGE	--	-0.62	-0.02	**0.19**	--	-0.06	0.33	**0.42**
Yield (t/ha)	Mean	3.88	3.05	**3.68**	**3.68**	4.56	2.62	**3.51**	3.43
	MAB	--	0.25	**0.15**	0.19	--	0.70	**0.30**	0.29
	RMSE	--	1.19	**0.77**	0.93	--	3.82	1.70	**1.64**
	r	--	0.27	**0.38**	0.30	--	-0.76*	-0.04	**0.16**
	KGE	--	0.12	**0.26**	0.10	--	-1.06	-0.17	**-0.04**
Growing season length (days)	Mean	129	69	**126**	136	117	**114**	123	121
	MAB	--	0.47	**0.11**	**0.10**	--	**0.07**	**0.08**	0.10
	RMSE	--	62.84	**15.62**	**15.44**	--	**11.3**	12.02	15.24
	r	--	0.37	**0.66***	**0.62***	--	0.25	**0.40**	-0.07
	KGE	--	-0.21	**0.57**	0.52	--	0.21	**0.39**	-0.07
	Overall bias	--	0.51	0.26	**0.24**	--	0.48	0.26	**0.25**

* significant at p<.05 using the students t-test. The bold font indicates the best performer in each category; if multiple models are marked in bold font, that indicates a lack of statistically significant difference between them.

3.1.2.2 Yield

The CLM5_Def yield of 2.62 t/ha is much lower than the observed 4.56 t/ha (Table 3). The mean yield improved by nearly 1 t/ha in the CLM5_Mod runs but is still lower than observations. The MAB improved from 0.699 in the CLM5_Def case to 0.297 in the CLM5_Mod1 case and 0.291 in the CLM5_Mod2 case. The most significant improvement from CLM5_Def to CLM5_Mod cases is in rice yield predictions (Table 3). RMSE improved from 1.63 t/ha in CLM5_Def to 0.65 t/ha in CLM5_Mod1 and 0.53 t/ha in CLM5_Mod2. Similarly, *r*-value improved from -0.76 in CLM5_Def to -0.04 in CLM5_Mod1 and 0.16 in CLM5_Mod2. KGE has the best value of -0.04 in CLM5_Mod2, which is far from perfect but is much better than -1.06 in CLM5_Def and -0.17 in CLM5_Mod1. The improvement from CLM5_Mod1 to CLM5_Mod2 is significant (p<.01), especially in terms of *r*-value and KGE.

Figure 4(b.2) highlights the significant improvement made through CLM5_Mod1 and CLM5_Mod2 in reducing the bias at all sites. The bias in CLM5_Mod1 overlaps the bias in CLM5_Mod2 at Raipur, Kuthulia, Jabalpur, Faizabad, Pantnagar, and Kaul. The bias in CLM5_Mod1 and CLM5_Mod2 are identical at all the above-mentioned sites. Therefore, introducing latitudinal variation in CLM5_Mod2 has a significant impact on improving LAI simulation at all sites (Figure 4(a.2)) and has simulated yield better than the CLM5_Mod1, especially in the southern region (Anantapur and Hyderabad) (Figure 4(b.2) and Figure S6).
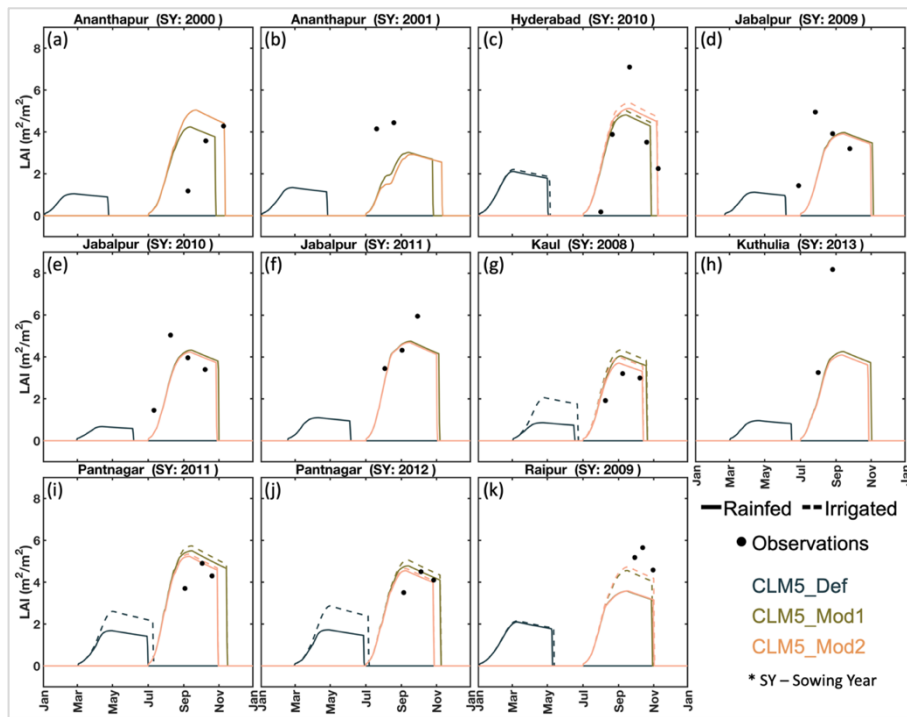
Figure 5: Site scale LAI simulated by three versions of CLM5 against observations for rice.

3.1.2.3 Growing Season Length

The CLM5_Def model performed exceptionally well in simulating the growing season length with a value of 114 days, which
430   is closest to the observed value of 117 days (Table 3). The MAB and the RMSE in the default case are the lowest, even though
the MAB shows no significant difference among the three CLM5 versions. During our bootstrap exercise with 10000 samples,
no significant difference between MAB among the three setups was observed. RMSE in CLM5_Mod1 is lower than
CLM5_Mod2. The *r*-value in CLM5_Mod2 (-0.07) shows no variation in growing season length among the sites. However,
Figure 5 shows that the longer or shorter growing season lengths observed at the site scale are simulated in CLM5_Mod2.
435   Figure 4(c.2) shows that no version of the CLM5 model is outperforming the others in simulating the growing season length
of rice. Additionally, bias in all models is very low, less than 0.2 in most sites.

The overall bias in Table 3 and Figure S4 for rice shows that the CLM5_Mod2 is performing significantly better than the other
CLM5 versions. Using latitudinal variation in base temperature for rice improved the LAI and yield at all sites (Figure 4,
440   Figure 5, Figure S4, and Figure S6). This suggests that latitudinal variation in base temperature implemented in the
CLM5_Mod2 is necessary to capture the growth variation observed across Indian rice growing regions.

3.2 Outcome of model improvements at the regional scale
3.2.1 Yield

Figure 6 compared regional-scale yield simulations by CLM5 against the EarthStat data (Ray et al., 2012). CLM5_Def simulations underestimated the wheat yield in central and south-central regions of the wheat growing regions, which is also identified by Lombardozzi et al. (2020). In the CLM5_Mod1 case, the underestimation found by Lombardozzi et al. (2020) reduced, but at the same time, an overestimation of yield is observed in the eastern parts of the wheat-growing regions. The overestimation is reduced by introducing latitudinal variation in the CLM5_Mod2 case. Large parts of the wheat-growing regions have a low bias between -1 and 1 ton per hectare compared to the EarthStat data. One important region where CLM5_Mod2 is underestimating is the Punjab and Haryana regions (the northwest region in the map). In Figure S7, we compare the total annual yield from wheat-growing regions simulated by CLM5 with the FAO data. CLM5_Mod1 replicates the trend observed in FAO data. CLM5_Def underestimated the total yield owing to the lower growing season simulated in the default case.
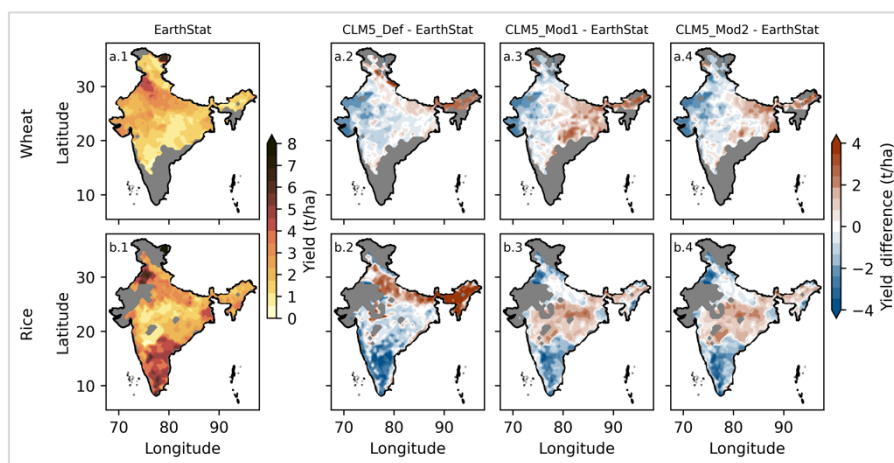
Figure 6: Yield estimates of (a) wheat and (b) rice by (1) EarthStat 2005, and (2-4) difference in yield between CLM5 (mean 2003-2007) versions and EarthStat data.

The CLM5_Def rice simulations underestimated the yield across large parts of the rice-growing regions and overestimated it in the Indo-Gangetic Plains (IGP) and northeast regions. CLM5 simulated a higher yield in IGP, which has a comparatively lower rice growing area than in the central and eastern parts of India (Figure S8). Improved yield simulation is observed in the CLM5_Mod1 case due to changes in the growing season and grain fill threshold. The overestimation in IGP and the underestimation in southern parts of India decreased (Figure 6(b.3)). However, changes made in the CLM5_Mod2 case showed slight improvement in most regions over the CLM5_Mod1 case (Figure 6(b.3) and 6(b.4)). In CLM5, rice is grown only during the Kharif season; however, in the southern regions of India, where water is available throughout the year, rice is grown in two or three seasons (Wang et al., 2022). Therefore, the annual yield observations in EarthStat are higher in this region and are not reflected in the CLM5 simulations. In Figure S7(b), we compared the annual rice yield over rice-growing regions of India from CML5 simulations and FAO data. CLM5_Def overestimated the yield, considering the fact that rice is growing in only one season in CLM5. With the improvements made in CLM5, the trend in FAO is matched by the modified simulations, however,

yield in modified cases is lower compared to FAO data across the fifteen years. The underestimation in yield is expected because rice grows in only one season in CLM5.

470 The improvement in rice crop growth and yield is twofold in this study. One is changing the growing season, and the other is the grainfill parameter. A study by Rabin et al. (2023) used the CLM5 model to simulate crop yields of major crops across the globe. The important point to note here is that they used a prescribed calendar; therefore, the growing season is accurate for crops in all regions, but they did not change the grain fill parameter and used the default value of 0.4. The results for rice yield were poor compared to the FAO data (Rabin et al., 2023). Therefore, changing the growing season would not improve the

475 yield of rice crops. Our sensitivity studies with the grain fill parameter showed that the value 0.65 produced better crop growth and yields after changing the growing season. The underestimation of yield for wheat and rice pointed out by Lombardozzi et al. (2020) is reduced to some extent with the modifications in this study. In the default case, bias in yield, especially in rice, is around ±3 t/ha, which is reduced in CLM5_Mod2 to ±1.5 t/ha. However, more research is required to understand the reason for the bias in CLM5_Mod cases in the range of ±1.5 t/ha in both rice and wheat.

480 **3.2.2 Irrigation**

We compared our simulated irrigation across wheat and rice-growing regions of India against the annual irrigation patterns from Biemans et al. (2016). In Figure 7, the blue line shows the annual irrigation pattern simulated by Biemans et al. (2016), the black line depicts irrigation simulated by the CLM-Def case, and the green and orange lines show the CLM5_Mod1 and CLM5_Mod2 simulations, respectively. CLM5_Def has anomalous peaks in the pre-monsoon summer season for wheat and

485 rice. These are also found in Mathur and AchuthaRao. (2019). This error in irrigation seasonality resulted from wrong cropping patterns of wheat and rice in India in the CLM5_Def case. The modified CLM5 simulations matched the patterns from Biemans et al. (2016). One significant difference between the current study and Biemans et al. (2016) is that the rice is grown in the rabi and kharif seasons in Biemans et al. (2016), while in our study, rice is sown in only the Kharif season. CLM5 is not currently equipped to simulate multiple crop sowings in a year, and the rainfed and irrigated rice crop maps of CLM5 (Figure

490 S8) do not reflect the kharif and rabi rice crop maps. Another important point to note is that Biemans et al. (2016) reported the total irrigation water demand of the crop during the growing season, and we are comparing it with water added through irrigation to the crops.

The improvements made in our study improved the seasonality of the irrigation in wheat and rice croplands. The improved models simulate less water added through irrigation for the wheat and rice crops. Water added through irrigation over the

495 wheat growing region is reduced from 4.32 billion cubic meters/day (BCM/day) in CLM5_Def to 3.08 BCM/day in CLM5_Mod1 and 3.53 BCM/day in CLM5_Mod2. The drastic difference in irrigation water added is because wheat is now growing in the rabi season in the Mod cases compared to the summer season in CLM5_Def. A more significant reduction in irrigation water added to crops is observed in the case of rice. CLM5_Def simulates 8.09 BCM/day of water added through irrigation, while CLM5_Mod1 and CLM5_Mod2 simulates only 2.97 and 3.09 BCM/day, respectively. Such drastic

500 differences in water added through irrigation will significantly impact the hydrological cycle.
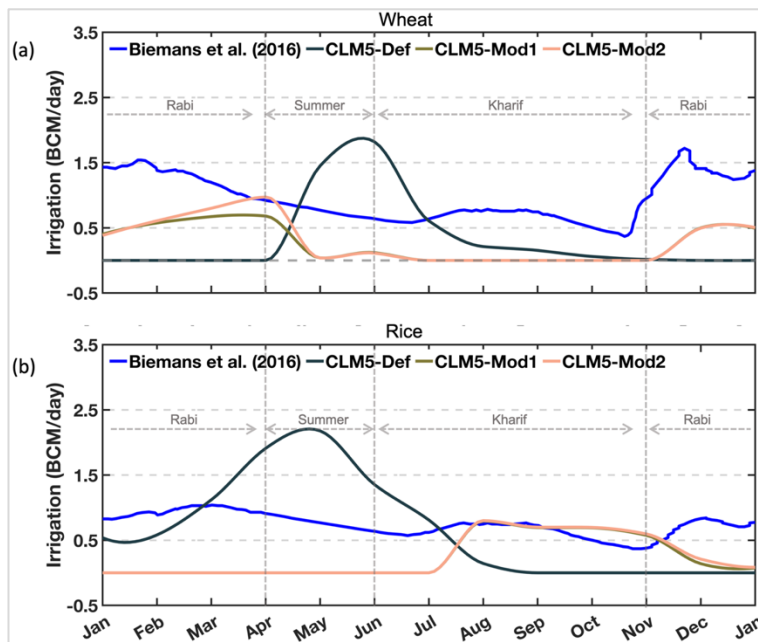
Figure 7: Comparison of water added through irrigation simulated by CLM5 and water demand data from Biemans et al. (2016).

3.2.3 GPP and LAI

3.2.3.1 Spatiotemporal variation

505   The monthly spatial patterns of simulated GPP and LAI are shown in Figures 8 and 9. The primary crop-growing months are June till March. This is evident in the MODIS GPP and LAI observations. However, the CLM5_Def simulated low GPP and LAI during this period. This is due to the error in the crop calendar in the default model. CLM5_Def simulated maximum carbon uptake (GPP) and LAI in April and May (Figure 8: Apr and May) when very little vegetation activity is observed across India, which is also evident from MODIS GPP and LAI data (Figure 9: Apr and May). In contrast, the modified models

510   simulated the GPP and LAI cycle as observed in the MODIS data with high GPP and LAI during June-March and low values during the rest of the year.

The maximum observed GPP in the MODIS data is in the northeast and peninsular regions of India. In contrast, the maximum GPP simulated by CLM5_Def is in the IGP region. The CLM5_Mod1 and CLM5_Mod2 simulations are similar to the MODIS observations with maximum LAI in central and eastern parts of the country from July to February months of the year. Even

515   though the modified models captured the observed spatial patterns, they tend to overestimate the magnitudes.
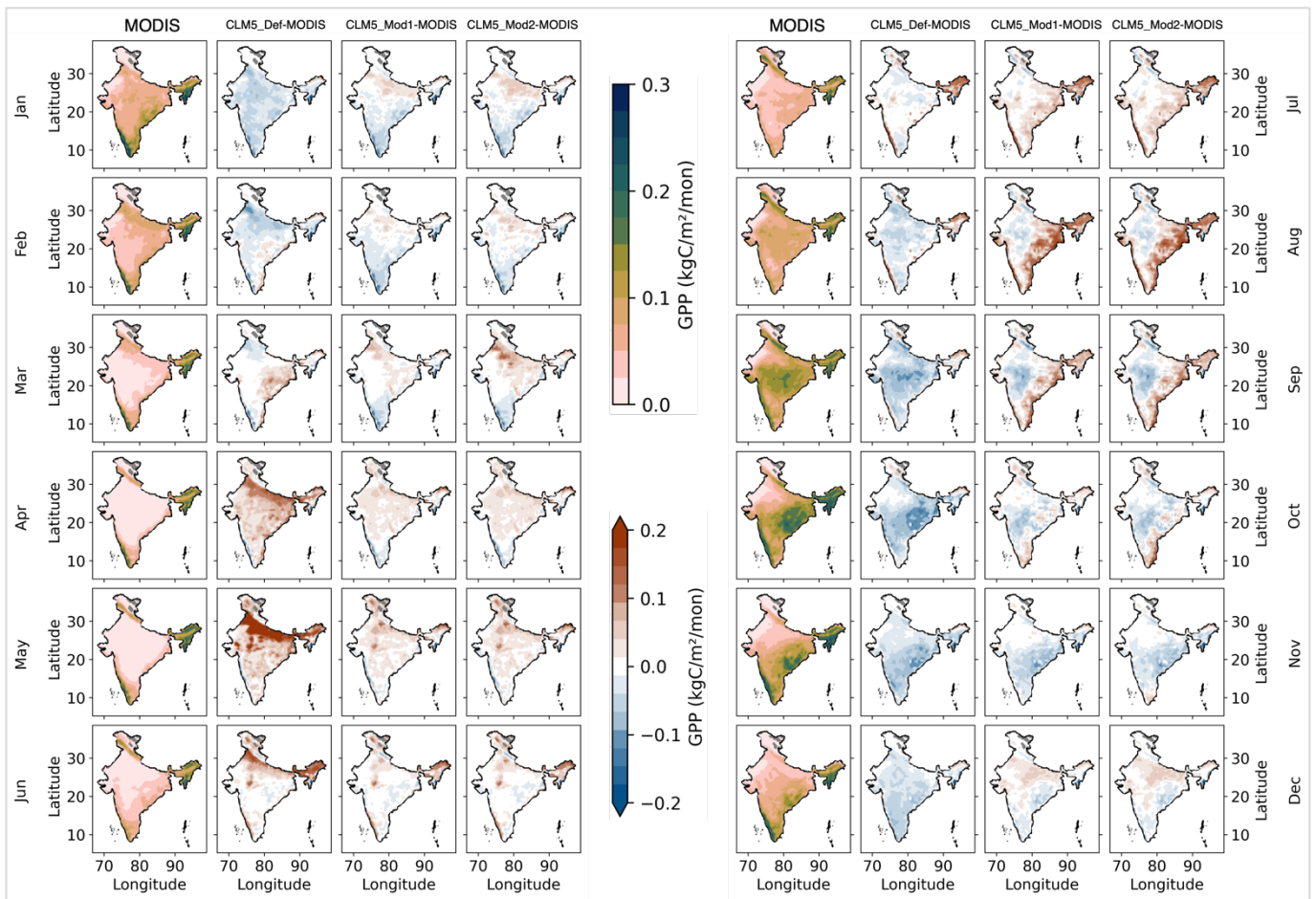
Figure 8: Spatial variation of GPP simulated by CLM5 against MODIS data. The data shows the monthly GPP averaged over 2000-2014.

3.2.3.2 Monthly time series

We evaluated the monthly time series of GPP and LAI from 2000 to 2014 (Table 4; Figure S9). The simulated GPP performed better in the modified versions of CLM5 than the default one. The monthly mean GPP has an MAB of 0.51 in CLM5_Def, 0.241 in CLM5_Mod1, and 0.235 in CLM5_Mod2. The RMSE decreased from 6.95 kgC/m^2/mon in CLM5_Def to 3.48 kgC/m^2/mon in Mod1 and 3.56 kgC/m^2/mon in Mod2. The most significant improvement in the model simulations is seen in the correlation of CLM5 simulated GPP against the MODIS observations. The *r*-value is negative in the case of CLM5_Def (-0.47) because the seasonality of vegetation growth in the Indian region is incorrect. The *r*-value improved to 0.76 in CLM5_Mod1 and CLM5_Mod2. Similarly, KGE has a negative value (-0.48) in CLM5-Def and improved to 0.72 in CLM5_Mod1 and 0.71 in CLM5_Mod2.
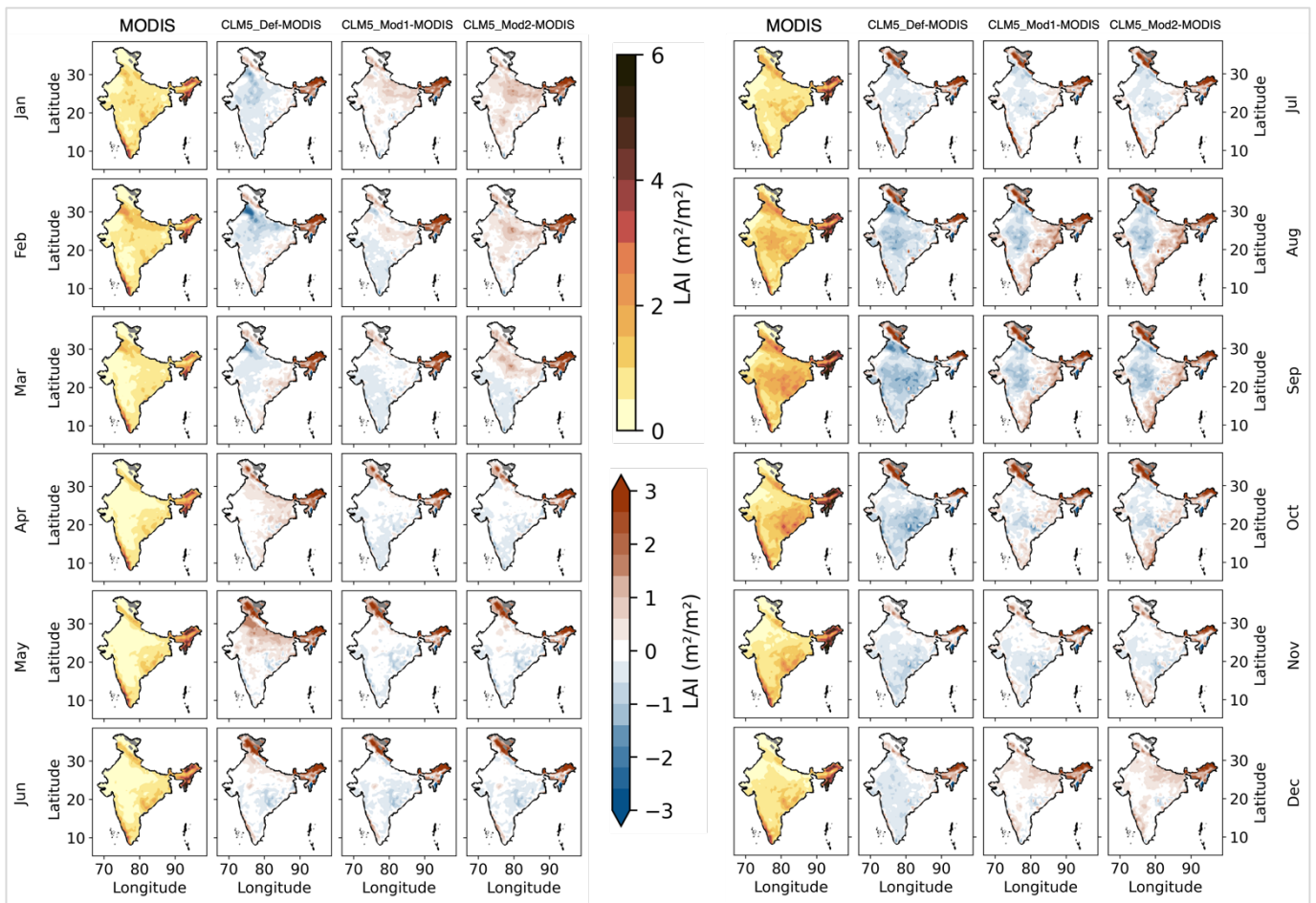
Figure 9: Spatial variation of LAI simulated by CLM5 against MODIS data. The data shows the monthly LAI averaged over 2000-2014.

The peaks in annual GPP from 2001 to 2014 (in Figure S9(a)) in the case of CLM5_Def are off by at least three months compared to MODIS GPP, while the peaks in CLM5_Mod1 and CLM5_Mod2 are consistent with the observations. Figure 10(b) shows the monthly GPP comparison of CLM5 simulations against MODIS data in a Taylor Diagram. Higher correlation, lower RMS error, and smaller standard deviation characterize the most accurate CLM5 configuration, as seen in the closer proximity of CLM5_Mod2 markers to the observational reference point. A drastic improvement is observed from default to modified cases; the correlation improved along with standard deviation, which got very close to observations (black star on Taylor Diagram) in the modified cases. CLM5_Mod2 is the best-performing setup in Figure 10(b), with high correlation and low standard deviation.

Interestingly, not all evaluation metrics for LAI improved with changes made to CLM5 in this study. The monthly mean LAI had an MAB of 0.19 in the CLM5_Def case, 0.24 in the CLM5_Mod1 case, and 0.3 in the CLM5_Mod2 case. RMSE in

CLM5_Def is 0.27 m²/m², which increased to 0.29 m²/m² in the CLM5_Mod1 case and 0.35 m²/m² in the CLM5_Mod2 case. The overestimation of LAI is consistent across all CLM5 simulations (Figure S9(b)). The overestimation of LAI by process-
545 based vegetation models compared to MODIS LAI data is widely reported (Fang et al., 2019). The reasons are processes like carbon fixation and allocation of biomass to leaves in the models (Gibelin et al., 2006; Richardson et al., 2012), differences in defining the LAI by various models and MODIS (Fang et al., 2019), and due to inherent bias in LAI estimation in MODIS in the equatorial region (20 °S to 15 °N) (Fang et al., 2019; Lin et al., 2023). Figure S9(b) illustrates that although the bias is higher in Mod cases, the peaks in annual LAI in MODIS data are captured accurately by the Mod cases. The CLM5_Def peak
550 in LAI is off by two to three months.

Table 4: Evaluation of CLM5 simulations at the regional scale against MODIS (LAI and GPP) and FLUXCOM (LH and SH) data. The bold text states that the version of CLM5 is performing the best.

Parameter	Evaluation Metrics	CLM5_Def	CLM5_Mod1	CLM5_Mod2
GPP	MAB	0.51	0.24	**0.24**
	RMSE	6.95	**3.48**	3.56
	r	-0.47*	0.76*	**0.76***
	KGE	-0.48	**0.72**	0.71
LAI	MAB	**0.19**	0.24	0.31
	RMSE	**0.27**	0.29	0.35
	r	0.35*	0.92*	**0.93***
	KGE	0.34	0.40	**0.41**
LH	MAB	0.22	0.17	**0.16**
	RMSE	14.78	11.91	**11.28**
	r	0.69*	0.93*	**0.93***
	KGE	0.60	0.77	**0.77**
SH	MAB	0.22	**0.19**	0.20
	RMSE	14.34	**11.16**	11.56
	r	0.85*	0.94*	**0.95***
	KGE	0.52	0.73	**0.73**

* significant at p<.01 using the students t-test

Other evaluation metrics of LAI showed that the modified models are performing much better than the default case. The *r*-
555 value in CLM5_Def is 0.35, which increased to 0.92 in the CLM5_Mod1 case and 0.93 in the CLM5_Mod2 case. Higher *r* values in modified runs imply that the seasonality of LAI simulated by CLM5 considerably improved due to the improvements made in the model. KGE metric showed improvement from 0.35 in the CLM5_Def case to 0.4 in the CLM5_Mod1 case and to 0.41 in the CLM5_Mod2 case (Table 4). The Taylor diagram of LAI (Figure 10(a)) showed improvement in correlation, but the error and standard deviation are higher than the observations.

560 **3.3 Heat fluxes**

3.3.1 Latent Heat flux

3.3.1.1 Spatial variation

The spatial and monthly variation in the CLM5 simulation of LH is illustrated in Figure S10. Most of the spatial pattern in observed LH is captured by all setups of the CLM5 model. However, one error in the case of CLM5_Def is observed in March, April, and May, where the IGP region shows high LH values absent in FLUXCOM observations. This erroneous high LH in this region is due to the wheat growth evident from Figure 9. The least LH is observed during the winter months, November to February, across all CLM5 simulations.

3.3.1.2 Monthly time series

Comparing the latent heat flux (LH) simulated by CLM5 with FLUXCOM data, we observe MAB of the LH reduced from 0.22 in CLM5_Def to 0.27 in CLM5_Mod1 and 0.16 in CLM5_Mod2. The RMSE reduced from 14.74 W/m^2 in the CLM5_Def to 11.91 W/m^2 in CLM5_Mod1 and 11.28 W/m^2 in CLM5_Mod2. The correlation improved from 0.69 in CLM5_Def to 0.93 in CLM5_Mod1 and CLM5_Mod2 cases. KGE metric improved from 0.70 in CLM5_Def to 0.77 in CLM5_Mod cases. The improvement is evident in the Taylor diagram (Figure 10(c)). CLM5_Mod simulations are much closer to the observations than the CLM5_Def case. CLM5_Mod1 and CLM5_Mod2 have similar performance, even though LAI improved in CLM5_Mod2 over CLM5_Mod1. Figure S12(a) depicts that the CLM5 simulations underestimate the LH compared to FLUXCOM data.
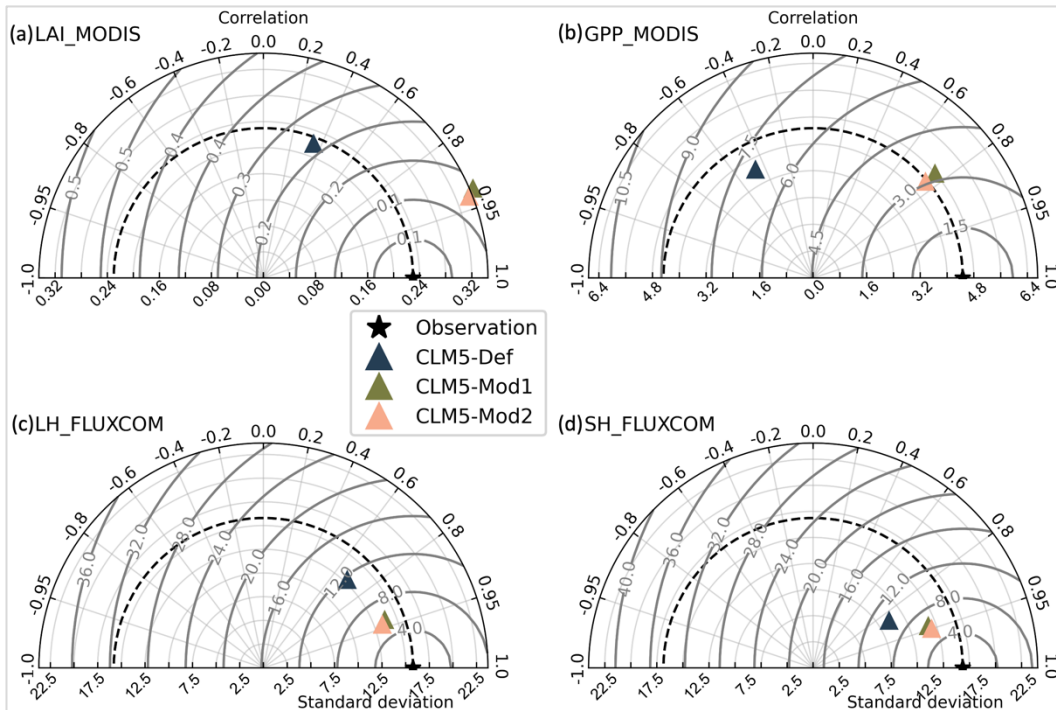
Figure 10: Comparing CLM5 simulated (a) LAI, (b) GPP, (c) LH, and (d) SH against observations. The data used here is the monthly mean from 2000 to 2014.

3.3.2 Sensible Heat flux

3.3.1.1 Spatial variation

The spatial and monthly variation in the CLM5 simulation of SH is illustrated in Figure S11. Most of the spatial pattern in observed SH is captured by all setups of the CLM5 model. However, CLM5_Def simulated slightly lower SH than the modified model simulations, especially from March to June. Low SH is observed from August to December across all CLM5 simulations.

3.3.2.2 Monthly time series

Comparing the sensible heat flux (SH) simulated by CLM5, we observed the MAB of SH reduced from 0.22 in CLM5_Def to 0.19 in CLM5_Mod1 and 0.20 in CLM5_Mod2. The RMSE reduced from 14.34 W/m^2 in CLM5_Def to 11.16 W/m^2 in CLM5_Mod1. The RMSE in CLM5_Mod2 is 11.56 W/m^2, slightly higher than in the CLM5_Mod1 case. The correlation improved from 0.85 in CLM5_Def to 0.94 in CLM5_Mod1 and 0.95 in CLM5_Mod2. KGE metric improved from 0.52 in CLM5_Def to 0.73 in CLM5_Mod cases. The SH in CLM5 is affected by vegetation temperature and ground temperatures. The results suggest that a difference in vegetation temperatures is observed between CLM5_Def and CLM5_Mod1, and very little to no difference is observed between CLM5_Mod1 and CLM5_Mod2. The difference in vegetation temperature is likely caused by the accurate representation of the growing season in CLM5_Mod cases compared to CLM5_Def. This is also evident from the Taylor diagram (Figure 10(d)), where we see improvement from CLM5_Def to CLM5_Mod1, but CLM5_Mod1 and CLM5_Mod2 markers overlap. Figure S12(b) depicts that the CLM5 simulations underestimated the highs and lows of SH in FLUXCOM data. The peak of SH in all CLM5 simulations is in line with the FLUXCOM data. However, CLM5_Def has a larger bias in estimating the maximum SH during a year.

Overall, the improvements in the representation of the two major Indian crops drastically improved the surface energy flux simulations by CLM5 (Figure 10b, c, and d).

4 Discussions

In this study, we improved the representation of wheat and rice, the two major crops grown in India, in the CLM5 land model. One major strength of the current study is using multiple site-scale observations for calibrating and validating the crop modules in CLM5. Studies such as those by Gahlot et al. (2020), who looked at Indian crops, used only one site for calibrating and evaluating their model. Even studies carried out for winter wheat across the globe (Lokupitiya et al., 2009; Lu et al., 2017; Boas et al., 2021) used two or three sites for calibrating the model. In contrast, we used 33 growing seasons from 14 sites, resulting in a rigorous calibration and evaluation exercise. The improved model in our study not only simulated crop phenology better but also improved the simulation of energy and water fluxes. The results demonstrate the importance of accurate representation of crops in land surface models, especially in a country like India, where more than 50% of land is used for agriculture.

This study looked at the variability in yield simulations at a regional scale for two major Indian crops. When compared against the EarthStat 2005 yield data, few regions showed improvement from the default CLM5 version to the modified version. Nevertheless, the yield simulated by CLM5 for wheat and rice needs improvement. Yield is now calculated as the available dry matter allocated to the grain after the allocation to root, leaf, and stem. Global studies like Rabin et al. (2023) highlighted

the issue of inconsistent improvement in yield estimates at different scales while analyzing the inter-annual and spatial variation in yield estimates. A recent study by Yin et al. (2024), which looked at the yield estimates by various models, concluded that the CLM5 simulated the temporal variability well but failed to simulate the spatial variability across China's wheat and rice-growing regions. Similarly, in our study, we found an improvement in site-scale yield estimates over different growing seasons but found mixed results in regional yield estimates. The yield should perform better since the CLM5 simulates the GPP with lower bias and improved seasonality. However, that is not the case here. Therefore, an investigation into the yield estimation, especially wheat in CLM5, is necessary.

A region with significant agricultural coverage and practices is misrepresented in the most widely used land surface model. Our study improved the model representation of the two major Indian crops. Our future goal is to study the feedback in the land-atmosphere system using the improved land model. The enhanced crop representation and management practices will impact the water cycle and local and global temperature and precipitation (Mathur and Rao, 2020). Rice and wheat constitute 80% of India's harvested land area, followed by maize, sugarcane, and cotton. Improving parameterizations for all these Indian crops (seasonal and cash crops) would be an ideal next step.

While our study made progress in correcting shortcomings, it is critical to recognize that the CLM5 model, like any sophisticated climate model, is still a work in progress. Future improvements should address broader model deficiencies highlighted in ours and various other studies. The deficiencies range from the inclusion of sophisticated plant and soil hydraulics (Boas et al., 2021; Raczka et al., 2021), improvement in yield predictions, improved or new management practices like tillage (Graham et al., 2021), post-harvest crop residual management. Furthermore, our research contributes to continuing attempts to improve the CLM5 model by addressing shortcomings in Indian crop representation. The enhancements are a step forward, emphasizing the iterative nature of model development and the importance of constant refinement to ensure the accuracy of the model in replicating complex earth system processes. Future studies should build on these findings, including additional enhancements to address broader shortcomings in the model.

The major drawback of this study is that it does not consider the multiple croppings of rice followed in major parts of India. Although the harvested area of rice grown in rabi and summer seasons is very low (Biemans et al., 2016), it is important to include the rice growth in these seasons in LSMs. This will significantly impact the terrestrial fluxes at the local scale (Oo et al., 2023). The lower LH simulated by the CLM5 models during the rabi and summer season (November to June) compared to FLUXCOM data (Figure S12(a)) might be due to growing rice in kharif season only. However, because of the small areal coverage of rabi and summer rice, their impact on large scale fluxes and weather/climate is likely to be small. This study did not consider other major crops, such as maize, soybean, and pulses, which cover substantial harvesting areas. Future studies should focus on improving the representation of these crops in CLM5 for a comprehensive study of climate impacts on Indian agroecosystems.

5 Conclusion

Two major modifications were made to CLM5 in this study. First, the representation of wheat and rice growing seasons in India was improved to align better with the observations. Second, a latitudinal variation in base temperature was implemented to capture the crop varieties grown across diverse Indian agro-climatic conditions. These modifications resulted in the following improvements in the CLM5 simulations:

- The crop phenology is realistic in the modified models. The models simulate rice and wheat growth in the seasons they are grown in the field.
- The LAI simulations are significantly better in wheat and rice at the site scale—the bias in the simulations reduced by nearly 50% compared to the default model.
- The simulated growing season length for wheat is significantly better at the site scale. The rmse improved from over 60 days in the default model to just over 15 days.
- The simulations of rice yield are significantly better at both site and regional scales.
- The carbon uptake (GPP) simulations over the Indian region are significantly better, improving from a negative correlation in the default model to a high positive correlation.
- The seasonality of simulated irrigation patterns across crop regimes in India is realistic.

Irrigation is a significant part of agriculture in India. With the improvements made to the model, irrigation patterns improved drastically and are now in line with a study by Biemans et al. (2016). The amount of water taken up by the crops through irrigation during their respective growing seasons decreased, and at the same time, the latent heat simulations improved from the default case.

CLM5 defines its crop parameters globally and, therefore, has a significant bias in regions such as India, where crop practices are unlike those in Europe or North America. This study demonstrated that the global land models must use region-specific parameters rather than global ones for accurately simulating vegetation and land surface processes. Such improved land models will be a great asset in investigating the global and regional scale land-atmosphere interactions and developing improved future climate scenarios. Models that can simulate regional crop and land processes accurately will be able to predict the future water demand of the crops and if enough water sources are available to meet the needs. They can also help in providing estimates of productivity and net carbon capture abilities of agroecosystems in future climate.

Code and data availability: The site scale data used in the study is available at Varma et al. (2024). The code changes made in CLM5, domain, surface, and land use time series data used for the site scale and regional simulations are available at https://doi.org/10.5281/zenodo.14040383 Reddy et al. (2024). The Python codes and the data used to generate the figures are available at https://doi.org/10.5281/zenodo.14040383 Reddy et al. (2024).

Author Contribution: KNR and SBR conceptualized the study. KNR, SBR, SSR, and DLL designed the methodology. KNR conducted the experiments. KNR made changes to the code with the guidance from SSR. GVV and RB compiled the site scale data. RB conducted a few site-scale base-temperature sensitivity experiments. DCN generated CLM input files required for

experiments. KNR analyzed the results and wrote the manuscript. SSR and DLL reviewed the manuscript. SBR edited the paper.

Competing Interests: At least one of the (co-)authors is a member of the editorial board of Geoscientific Model Development.

References

Asseng, S., Cammarano, D., Basso, B., Chung, U., Alderman, P. D., Sonder, K., Reynolds, M., and Lobell, D.B.: Hot spots of wheat yield decline with rising temperatures. Glob. Change Biol., 23(6), pp.2464–2472, https://doi.org/10.1111/gcb.13530, 2017.

Biemans, H., Siderius, C., Mishra, A., and Ahmad, B.: Crop-specific seasonal estimates of irrigation-water demand in South Asia, Hydrol. Earth Syst. Sci., 20, 1971–1982, https://doi.org/10.5194/hess-20-1971-2016, 2016.

Blyth, E. M., Arora, V. K., Clark, D. B., Dadson, S. J., de Kauwe, M. G., Lawrence, D. M., Melton, J. R., Pongratz, J., Turton, R. H., Yoshimura, K., and Yuan, H.: Advances in Land Surface Modelling, Curr. Clim. Change Rep.-2021, 7:2, 7(2), 45–71. https://doi.org/10.1007/S40641-021-00171-5, 2021.

Boas, T., Bogena, H., Grünwald, T., Heinesch, B., Ryu, D., Schmidt, M., Vereecken, H., Western, A., and Hendricks Franssen, H.-J.: Improving the representation of cropland sites in the Community Land Model (CLM) version 5.0, Geosci. Model Dev., 14, 573–601, https://doi.org/10.5194/gmd-14-573-2021, 2021.

Boas, T., Bogena, H. R., Ryu, D., Vereecken, H., Western, A., and Hendricks Franssen, H.-J.: Seasonal soil moisture and crop yield prediction with fifth-generation seasonal forecasting system (SEAS5) long-range meteorological forecasts in a land surface modeling approach, Hydrol. Earth Syst. Sci., 27, 3143–3167, https://doi.org/10.5194/hess-27-3143-2023, 2023.

Chen, M., Griffis, T. J., Baker, J. M., Wood, J. D., Meyers, T., and Suyker, A.: Comparing crop growth and carbon budgets simulated across AmeriFlux agricultural sites using the Community Land Model (CLM), Agr. Forest Meteorol., 256–257, 315–333, https://doi.org/10.1016/j.agrformet.2018.03.012, 2018.

Cheng, Y., Huang, M., Chen, M., Guan, K., Bernacchi, C., Peng, B., and Tan, Z.: Parameterizing Perennial Bioenergy Crops in Version 5 of the Community Land Model Based on Site-Level Observations in the Central Midwestern United States, J. Adv. Model. Earth Syst., 12, e2019MS001719, https://doi.org/10.1029/2019MS001719, 2020.

Cheng, Y., Huang, M., Zhu, B., Bisht, G., Zhou, T., Liu, Y., Song, F., and He, X.: Validation of the Community Land Model Version 5 Over the Contiguous United States (CONUS) Using In-Situ and Remote Sensing Data Sets, J. Geophys. Res.-Atmos., 126, 1–27, https://doi.org/10.1029/2020JD033539, 2021.

Collier, N., Hoffman, F. M., Lawrence, D. M., Keppel-Aleks, G., Koven, C. D., Riley, W. J., Mu, M., and Randerson, J. T.: The International Land Model Benchmarking (ILAMB) System: Design, Theory, and Implementation, J. Adv. Model. Earth Syst., 10, 2731–2754, https://doi.org/10.1029/2018MS001354, 2018.

Denager, T., Sonnenborg, T. O., Looms, M. C., Bogena, H., and Jensen, K. H.: Point-scale multi-objective calibration of the Community Land Model (version 5.0) using in situ observations of water and energy fluxes and variables, Hydrol. Earth Syst. Sci., 27, 2827–2845, https://doi.org/10.5194/hess-27-2827-2023, 2023.

Elliott, J., Müller, C., Deryng, D., Chryssanthacopoulos, J., Boote, K. J., Büchner, M., Foster, I., Glotter, M., Heinke, J., Iizumi, T., Izaurralde, R. C., Mueller, N. D., Ray, D. K., C., Ruane, A. C., and Sheffield, J.: The Global Gridded Crop Model Intercomparison: data and modeling protocols for Phase 1 (v1.0), Geosci. Model Dev., 8, 261–277, https://doi.org/10.5194/gmd-8-261-2015, 2015.

Fang, H., Zhang, Y., Wei, S., Li, W., Ye, Y., Sun, T., and Liu, W.: Validation of global moderate resolution leaf area index (LAI) products over croplands in northeastern China, Remote Sens. Environ., 233, 111377, https://doi.org/10.1016/j.rse.2019.111377, 2019.

Fisher, R. A. and Koven, C. D.: Perspectives on the Future of Land Surface Models and the Challenges of Representing Complex Terrestrial Systems, J. Adv. Model. Earth Sy., 12, e2018MS001453, https://doi.org/10.1029/2018MS001453, 2020.

Fisher, R. A., Wieder, W. R., Sanderson, B. M., Koven, C. D., Oleson, K. W., Xu, C., Fisher, J. B., Shi, M., Walker, A. P., and Lawrence, D. M.: Parametric Controls on Vegetation Responses to Biogeochemical Forcing in the CLM5, J. Adv. Model. Earth Sy., 11, 2879–2895, https://doi.org/10.1029/2019MS001609, 2019.

Gahlot, S., Lin, T.-S., Jain, A. K., Baidya Roy, S., Sehgal, V. K., and Dhakar, R.: Impact of environmental changes and land management practices on wheat production in India, Earth Syst. Dynam., 11, 641–652, https://doi.org/10.5194/esd-11-641-2020, 2020.

Gibelin, A.-L., Calvet, J.-C., Roujean, J.-L., Jarlan, L., and Los, S. O.: Ability of the land surface model ISBA-A-gs to simulate leaf area index at global scale: comparison with satellite products, J. Geophys. Res., 111, 1–16, https://doi.org/10.1029/2005JD006691, 2006.

Gupta, H. V., Kling, H., Yilmaz, K. K., and Martinez, G. F.: Decomposition of the mean squared error and NSE performance criteria: Implications for improving hydrological modelling, J. Hydrol., 377, 80–91, https://doi.org/10.1016/j.jhydrol.2009.08.003, 2009. a

Graham, M. W., Thomas, R. Q., Lombardozzi, D. L., & O'Rourke, M. E.: Modest capacity of no-till farming to offset emissions over 21st century. Environ. Res. Lett., 16(5), 054055. https://doi.org/10.1088/1748-9326/abe6c6, 2021.

Jat, R. K., Singh, R. G., Kumar, M., Jat, M. L., Parihar, C. M., Bijarniya, D., Sutaliya, J. M., Jat, M. K., Parihar, M. D., Kakraliya, S. K., and Gupta, R. K.: Ten years of conservation agriculture in a rice–maize rotation of Eastern Gangetic Plains of India: Yield trends, water productivity and economic profitability. Field Crops Res., 232, pp.1–10, https://doi.org/10.1016/j.fcr.2018.12.004, 2019.

Jung, M., Koirala, S., Weber, U., Ichii, K., Gans, F., Camps-Valls, G., Papale, D., Schwalm, C., Tramontana, G., and Reichstein, M.: The FLUXCOM ensemble of global land-atmosphere energy fluxes, Sci. Data., in press, 6, https://doi.org/10.1038/s41597-019-0076-8, 2019.

Kling, H., Fuchs, M., and Paulin, M.: Runoff conditions in the upper Danube basin under an ensemble of climate change scenarios, J. Hydrol., 424–425, 264–277, https://doi.org/10.1016/j.jhydrol.2012.01.011, 2012. a

Kumar, B. S., Abdus, S., Nidhi, Sarath, C. M. A., Abburi Venkata, M. S. R., Narayanan, M., Saon, B., Jawahar L. C., Vijay G. M., Chandra B. S., Sandeep S. S., Kumar, S. V.: Critical weather limits for paddy rice under diverse ecosystems of India, Front. Plant Sci., 14, https://doi.org/10.3389/fpls.2023.1226064, 2023.

Lawrence, D. M., Fisher, R., Koven, C., Oleson, K., Svenson, S., Vertenstein, M. (coordinating lead authors), Andre, B., Bonan, G., Ghimire, B., van Kampenhout, L., Kennedy, D., Kluzek, E., Knox, R., Lawrence, P., Li, F., Li, H., Lombardozzi, D., Lu, Y., Perket, J., Riley, W., Sacks, W., Shi, M., Wieder, W., Xu, C. (lead authors), Ali, A., Badger, A., Bisht, G., Broxton, P., Brunke, M., Buzan, J., Clark, M., Craig, T., Dahlin, K., Drewniak, B., Emmons, L., Fisher, J., Flanner, M., Gentine, P., Lenaerts, J., Levis, S., Leung, L. R., Lipscomb, W., Pelletier, J., Ricciuto, D. M., Sanderson, B., Shuman, J., Slater, A., Subin, Z., Tang, J., Tawfik, A., Thomas, Q., Tilmes, S., Vitt, F., and Zeng, X.: Technical Description of version 5.0 of the Community Land Model (CLM), Natl. Cent. Atmospheric Res. (NCAR), available at: http://www.cesm.ucar.edu/models/cesm2/land/CLM50_Tech_Note.pdf (last access: 15 June 2020), 2018.

Lawrence, P., Lawrence, D. M., Hurtt, G. C., and Calvin, K. V.: Advancing our understanding of the impacts of historic and projected land use in the Earth System: The Land Use Model Intercomparison Project (LUMIP), AGU Fall Meeting 2019, San Francisco, USA, 9–13 December 2019, abstract: GC23B-01, 2019.

Levis, S., Bonan, G. B., Kluzek, E., Thornton, P. E., Jones, A., Sacks, W. J., and Kucharik, C. J.: Interactive Crop Management in the Community Earth System Model (CESM1): Seasonal Influences on Land-Atmosphere Fluxes, J. Climate, 25, 4839–4859, https://doi.org/10.1175/JCLI-D-11-00446.1, 2012.

Lin, W., Yuan, H., Dong, W., Zhang, S., Liu, S., Wei, N., Lu, X., Wei, Z., Hu, Y., and Dai, Y.: Reprocessed MODIS Version 6.1 Leaf Area Index Dataset and Its Evaluation for Land Surface and Climate Modeling, Remote Sens., 15, 1–25, https://doi.org/10.3390/rs15071780, 2023.

Lobell, D. B., Schlenker, W., and Costa-Roberts, J.: Climate Trends and Global Crop Production Since 1980, Science, 333, 616–620, https://doi.org/10.1126/science.1204531, 2011.

Lokupitiya, E., Denning, S., Paustian, K., Baker, I., Schaefer, K., Verma, S., Meyers, T., Bernacchi, C. J., Suyker, A., and Fischer, M.: Incorporation of crop phenology in Simple Biosphere Model (SiBcrop) to improve land-atmosphere carbon exchanges from croplands, Biogeosciences, 6, 969–986, https://doi.org/10.5194/bg-6-969-2009, 2009.

Lombardozzi, D. L., Lu, Y., Lawrence, P. J., Lawrence, D. M., Swenson, S., Oleson, K. W., Wieder, W. R., and Ainsworth, E. A.: Simulating Agriculture in the Community Land Model Version 5, J. Geophys. Res.-Biogeo., 125, e2019JG005529, https://doi.org/10.1029/2019JG005529, 2020.

775   Lu, Y., Williams, I. N., Bagley, J. E., Torn, M. S., and Kueppers, L. M.: Representing winter wheat in the Community Land Model (version 4.5), Geosci. Model Dev., 10, 1873–1888, https://doi.org/10.5194/gmd-10-1873-2017, 2017.

Lu, Y. and Yang, X.: Using the anomaly forcing Community Land Model (CLM 4.5) for crop yield projections, Geosci. Model Dev., 14, 1253–1265, https://doi.org/10.5194/gmd-14-1253-2021, 2021.

Ma, Y., Woolf, D., Fan, M., Qiao, L., Li, R., and Lehmann, J.: Global crop production increase by soil organic carbon, Nat.
780   Geosci., 16, 1159–1165, https://doi.org/10.1038/s41561-023-01302-3, 2023.

Mathur, R. and AchutaRao, K.: A modelling exploration of the sensitivity of the India's climate to irrigation, Clim. Dynam., 54, 1851–1872, https://doi.org/10.1007/s00382-019-05090-8, 2019.

McDermid, S. S., Mearns, L. O. and Ruane, A. C.: Representing agriculture in Earth System Models: Approaches and priorities for development, J. Adv. Model. Earth Sy., 9, 2230–2265, https://doi.org/10.1002/2016MS000749, 2017.

785   Mehta, P., and Dhaliwal, L. K.: Agromet wheat app for estimation of phenology and yield of wheat under Punjab conditions. Int. J. Biometeorol., 67(3), pp.439-445, https://doi.org/10.1007/s00484-022-02423-x, 2023.

Myneni, R., Knyazikhin, Y., and Park, T.: *MODIS/Terra+Aqua Leaf Area Index/FPAR 8-Day L4 Global 500m SIN Grid V061*, NASA EOSDIS Land Processes Distributed Active Archive Center. Accessed 2024-04-01 from https://doi.org/10.5067/MODIS/MCD15A2H.061, 2021. [Data set].

790   Mukherjee, A., Wang, S. Y. S., and Promchote, P.: Examination of the climate factors that reduced wheat yield in Northwest India during the 2000s. Water, 11(2), p.343, https://doi.org/10.3390/w11020343, 2019.

Oo, A. Z., Yamamoto, A., Ono, K., Umamageswari, C., Mano, M., Vanitha, K., Elayakumar, P., Matsuura, S., Bama, K. S., Raju, M. and Inubushi, K.: Ecosystem carbon dioxide exchange and water use efficiency in a triple-cropping rice paddy in Southern India: A two-year field observation, Sci. Total Environ., 854, p.158541,
795   https://doi.org/10.1016/j.scitotenv.2022.158541, 2023.

Osborne, T., Gornall, J., Hooker, J., Williams, K., Wiltshire, A., Betts, R., and Wheeler, T.: JULES-crop: a parametrisation of crops in the Joint UK Land Environment Simulator, Geosci. Model Dev., 8, 1139–1155, https://doi.org/10.5194/gmd-8-1139-2015, 2015.

Rabin, S. S., Sacks, W. J., Lombardozzi, D. L., Xia, L., and Robock, A.: Observation-based sowing dates and cultivars
800   significantly affect yield and irrigation for some crops in the Community Land Model (CLM5), Geosci. Model Dev., 16, 7253–7273, https://doi.org/10.5194/gmd-16-7253-2023, 2023.

Raczka, B., Hoar, T. J., Duarte, H. F., Fox, A. M., Anderson, J. L., Bowling, D. R., and Lin, J. C.: Improving CLM5.0 biomass and carbon exchange across the Western United States using a data assimilation system, J. Adv. Model. Earth Sy., 13, e2020MS002421, https://doi.org/10.1029/2020MS002421, 2021.

805   Ray, D. K., Ramankutty, N., Mueller, N. D., West, P. C., and Foley, J. A.: Recent patterns of crop yield growth and stagnation. Nat. Commun., 3, 1293. https://doi.org/10.1038/ncomms2296, 2012.

Rao, B. B., Chowdary, P. S., Sandeep, V. M., Pramod, V.P., and Rao, V. U. M.: Spatial analysis of the sensitivity of wheat yields to temperature in India, Agric. For. Meteorol., 200, 192-202, https://doi.org/10.1016/j.agrformet.2014.09.023, 2015.

810   Reddy, K. N., Baidya Roy, S., and Rabin, S.: KNR8070/CLM5_IndianCrop_improvements: v1.1 (v1.1). Zenodo. https://doi.org/10.5281/zenodo.14040383, 2024. [Dataset]

Richardson, A. D., Anderson, R. S., Arain, M. A., Barr, A. G., Bohrer, G., Chen, G., Chen, J. M., Ciais, P., Davis, K. J., Desai, A. R., Dietze, M. C., Dragoni, D., Garrity, S. R., Gough, C. M., Grant, R., Hollinger, D. Y., Margolis, H. A., McCaughey, H., Migliavacca, M., Monson, R. K., Munger, J. W., Poulter, B., Raczka, B. M., Ricciuto, D. M.,
815   Sahoo, A. K., Schaefer, K., Tian, H., Vargas, R., Verbeeck, H., Xiao, J., and Xue, Y.: Terrestrial biosphere models need better representation of vegetation phenology: results from the North American Carbon Program Site Synthesis, Glob. Change Biol., 18, 566–584, doi:10.1111/j.13652486.2011.02562.x, 2012.

Ruiz-Vásquez, M. O. S., Arduini, G., Boussetta, S., Brenning, A., Bastos, A., Koirala, S., Balsamo, G., Reichstein, M. and Orth, R.: Impact of updating vegetation information on land surface model performance. J. Geophys. Res.-Atmos.,
820   128(21), https://doi.org/10.1029/2023JD039076, 2023.

Running, S. W. and Zhao, M.: User's Guide: Daily GPP and annual NPP(MOD17A2/A3)products, NASA Earth Observing System MODIS land algorithm 1–28, 2015.

Sacks, W. J., Deryng, D., Foley, J. A., and Ramankutty, N.: Crop planting dates: an analysis of global patterns, Global Ecol. Biogeogr., 19, 607–620, https://doi.org/10.1111/j.14668238.2010.00551.x, 2010.

825 Seo, H. and Kim, Y.: Forcing the Global Fire Emissions Database burned-area dataset into the Community Land Model version 5.0: impacts on carbon and water fluxes at high latitudes, Geosci. Model Dev., 16, 4699–4713, https://doi.org/10.5194/gmd-16-4699-2023, 2023.

Sheng, M., Liu, J., Zhu, A.-X., Rossiter, D. G., Zhu, L., and Peng, G.: Evaluation of CLM-Crop for maize growth simulation over Northeast China, Ecol. Model., 377, 26–34, https://doi.org/10.1016/j.ecolmodel.2018.03.005, 2018.

830 Song, J., Miller, G. R., Cahill, A. T., Aparecido, L. M. T., and Moore, G. W.: Modeling land surface processes over a mountainous rainforest in Costa Rica using CLM4.5 and CLM5, Geosci. Model Dev., 13, 5147–5173, https://doi.org/10.5194/gmd-13-5147-2020, 2020.

Strebel, L., Bogena, H. R., Vereecken, H., and Hendricks Franssen, H.-J.: Coupling the Community Land Model version 5.0 to the parallel data assimilation framework PDAF: description and applications, Geosci. Model Dev., 15, 395–411, 835 https://doi.org/10.5194/gmd-15-395-2022, 2022.

Su, Y.; Wu, J.; Zhang, C.; Wu, X.; Li, Q.; Liu, L.; Bi, C.; Zhang, H.; Lafortezza, R.; Chen, X. Estimating the Cooling Effect Magnitude of Urban Vegetation in Different Climate Zones Using Multi-Source Remote Sensing, Urban Clim., 43, 101155, https://doi.org/10.1016/j.uclim.2022.101155, 2022.

Taylor, K. E.: Summarizing multiple aspects of model performance in a single diagram, J. Geophys. Res., 106, 7183–7192, 840 2001

Thakur, S., Rana, R. S., and Manuja, S.: Thermal time requirement and yield of rice (Oryza sativa L.) under varying growing environments in changed climatic scenarios of Northwestern Himalayas, J. Pharm. Innov., SP-11(12), 35-38, 2022.

Tramontana, G., Jung, M., Schwalm, C. R., Ichii, K., Camps-Valls, G., Ráduly, B., Reichstein, M., Arain, M. A., Cescatti, A., Kiely, G., Merbold, L., Serrano-Ortiz, P., Sickert, S., Wolf, S., and Papale, D.: Predicting carbon dioxide and 845 energy fluxes across global FLUXNET sites with regression algorithms, Biogeosciences, 13, 4291–4313, https://doi.org/10.5194/bg-13-4291-2016, 2016.

Varma, G. V., Reddy, K. N., Baidya Roy, S., Yadav, R., Vangala, G., and Biswas, R.: Indian cereal crops (wheat and rice) phenology and agricultural management data across Indian croplands from 1960's to 2020. PANGAEA, https://doi.pangaea.de/10.1594/PANGAEA.964634, 2024. [Dataset]

850 Veeranjaneyulu, K.: KrishiKosh: an institutional repository of national agricultural research system in India, Libr. Manag., Vol. 35 Nos 4/5, pp. 345-354, https://doi.org/10.1108/LM-08-2013-008, 2014.

Wang, X., Folberth, C., Skalsky, R., Wang, S., Chen, B., Liu, Y., Chen, J., and Balkovic, J.: Crop calendar optimization for climate change adaptation in rice-based multiple cropping systems of India and Bangladesh, Agr. Forest Meteorol., 315, 108830, https://doi.org/10.1016/j.agrformet.2022.108830, 2022. a.

855 Yin, D., Li, F., Lu, Y., Zeng, X., Lin, Z., and Zhou, Y.: Assessment of Crop Yield in China Simulated by Thirteen Global Gridded Crop Models, Adv. Atmos. Sci., 41, 420–434, https://doi.org/10.1007/s00376-023-2234-3, 2024.

Yin, D., Yan, J., Li, F., Song, T.: Evaluation of global gridded crop models in simulating sugarcane yield in China, Atmos. Ocean. Sci. Lett., 16 (2), 100329, https://doi.org/10.1016/j.aosl.2023.100329, 2023.